Spectral and Condition Number Estimates of the Acoustic Single-Layer Operator for Low-Frequency Multiple Scattering in Dense Media*

Xavier Antoine† Bertrand Thierry†

Abstract

The aim of this paper is to derive spectral and condition number estimates of the single-layer operator for low-frequency multiple scattering problems. This work extends to dense media the analysis initiated in [6]. Estimates are obtained first in the case of circular cylinders by Fourier analysis and are next formally adapted to disks, ellipses and rectangles in the framework of boundary element methods. Numerical simulations validating the approach are also given.

1 Introduction

Integral equation techniques [12, 27] are an attractive and widely used tool to numerically solve acoustic, electromagnetic and elastic scattering problems. In particular, they can be used for multiple scattering configurations [25, 28] which have many applications in physics and mechanics [8, 14, 15, 16, 17, 20, 21, 24, 26]. A classical way to solve an integral equation is to use an iterative Krylov subspace solver (like e.g. the GMRES [29]) coupled to a Matrix-Vector acceleration scheme like the Fast Multipole Method [13, 18, 28]. A well-known property is that the convergence rate of the iterative solver is related to the condition number and spectral distribution of the integral equation. For this reason, understanding the spectral properties helps in building suitable preconditioners for integral equations. Spectral estimates have already been obtained for single scattering configurations. We refer to [4, 5, 6, 22, 23] for complete studies involving circular cylinders, convex and non convex structures [7, 10] as well as open surfaces or waveguides [2, 3, 11]. Multiple scattering problems are more complex in the sense that interactions between obstacles must be considered in the analysis. In a first part [6], we derived low-frequency spectral and condition number estimates of the single-layer potential for many distant obstacles (disks, ellipses and rectangles). The aim of this second part is to complete the previous results when the scatterers are close (dense media).

The plan of the paper is the following. In Section 2, we briefly introduce the single-layer operator and its spectral formulation. We also recall the analytical formula of the single-layer operator when the obstacle is a collection of circular cylinders. Section 3 explains how to obtain eigenvalues and condition number estimates of the single-layer operator for disks. Section 4 provides some

*The authors are partially supported by the French ANR fundings under the project MicroWave NT09_460489.

†Institut Elie Cartan Nancy, Université de Lorraine, CNRS UMR 7502, INRIA CORIDA Team, Boulevard des Aiguillettes B.P. 239, F-54506 Vandoeuvre-lès-Nancy, France (Xavier.Antoine@iecn.u-nancy.fr, Bertrand.Thierry@iecn.u-nancy.fr).

extensions of the results to circular, elliptical and rectangular cylinders in the framework of linear boundary element methods. Finally, Section 5 gives a conclusion and some perspectives.

2 The single-layer operator for multiple scattering by disks

We consider a homogeneous acoustic medium filling the whole space $\mathbb{R}^2$ and containing a bounded open set Ω with boundary $\Gamma := \partial\Omega$ such that the propagation domain $\mathbb{R}^2 \setminus \overline{\Omega}$ is connected. Throughout Sections 2 and 3, the set Ω is assumed to be a collection of M strictly disjoint (no sticky case) disks Ω_p with associated radii a_p and centers $\mathbf{O}_p$, for $p = 1, \ldots, M$. For two scatterers Ω_p and Ω_q, $1 \leq p \neq q \leq M$, we set $\mathbf{b}_{pq} = \mathbf{O}_q\mathbf{O}_p$, $b_{pq} = \|\mathbf{b}_{pq}\|$ and $\alpha_{pq} = \text{Angle}(\overrightarrow{Ox_1}, \mathbf{b}_{pq})$. For any real positive wave number k and smooth density $\rho \in H^{-1/2}(\Gamma)$, the single-layer integral operator is defined by

$$\forall \mathbf{x} \in \Gamma, \qquad L\rho(\mathbf{x}) = \int_\Gamma G(\mathbf{x}, \mathbf{y})\rho(\mathbf{y}) \mathrm{d}\Gamma(\mathbf{y}),$$

where the Green's function $G(\cdot\,, \cdot)$ is given by: $\forall \mathbf{x}, \mathbf{y} \in \mathbb{R}^2, \mathbf{x} \neq \mathbf{y}, G(\mathbf{x}, \mathbf{y}) = \frac{i}{4} H_0^{(1)}(k\|\mathbf{x} - \mathbf{y}\|)$ with $H_0^{(1)}$ is the zeroth order Hankel function of the first kind and $\|\mathbf{x}\| = (x_1^2 + x_2^2)^{1/2}$. The operator L is known [27] to be invertible from $H^{-1/2}(\Gamma)$ to $H^{1/2}(\Gamma)$ except for the set $F_D(\Omega)$ of Dirichlet irregular frequencies, that is the wave numbers k for which the interior homogeneous Dirichlet boundary value problem

$$\begin{cases} (\Delta + k^2)u = 0 & \text{in } \Omega \\ u = 0 & \text{on } \Gamma, \end{cases}$$

admits non trivial solution. Throughout this paper, we assume that $k \notin F_D(\Omega)$.

By introducing one Fourier basis per circular obstacle, we obtain [30] the following expression of the single-layer integral operator L as an infinite block matrix $\widetilde{\mathbb{L}}$ defined by

$$\widetilde{\mathbb{L}} = \begin{pmatrix} \widetilde{\mathbb{L}}^{1,1} & \widetilde{\mathbb{L}}^{1,2} & \ldots & \widetilde{\mathbb{L}}^{1,M} \\ \widetilde{\mathbb{L}}^{2,1} & \widetilde{\mathbb{L}}^{2,2} & \ldots & \widetilde{\mathbb{L}}^{2,1} \\ \vdots & \vdots & \ddots & \vdots \\ \widetilde{\mathbb{L}}^{M,1} & \widetilde{\mathbb{L}}^{M,2} & \ldots & \widetilde{\mathbb{L}}^{M,M} \end{pmatrix},$$

where each s infinite submatrix $\widetilde{\mathbb{L}}^{p,q} = (\widetilde{\mathbb{L}}^{p,q}_{m,n})_{m,n\in\mathbb{Z}}$ has for coefficients, for $m, n \in \mathbb{Z}$,

$$\widetilde{\mathbb{L}}^{p,q}_{m,n} = \begin{cases} \delta_{mn} \dfrac{i\pi a_p}{2} J_m(ka_p) H_m^{(1)}(ka_p) & \text{if } p = q, \\ \dfrac{i\pi\sqrt{a_p a_q}}{2} J_m(ka_p) S_{nm}(b_{pq}) J_n(ka_q) & \text{otherwise.} \end{cases} \tag{1}$$

Symbol δ_{mn} denotes the Krönecker's delta function, equal to 1 if $m = n$ and 0 otherwise. The quantity $S_{nm}(b_{pq})$ is given by: $S_{nm}(b_{pq}) = H^{(1)}_{n-m}(kb_{pq}) e^{i(n-m)\alpha_{pq}}$, for $p, q = 1, \ldots, M, p \neq q$ and $m, n \in \mathbb{Z}$. Let us remark that the infinite block $\widetilde{\mathbb{L}}^{p,p}$ located on the diagonal is a diagonal matrix whereas the off-diagonal block $\widetilde{\mathbb{L}}^{p,q}$, $p \neq q$, is a full matrix. Moreover, in the particular case of circular scatterers, we have $F_D := \{k > 0 / \exists (p, m) \in \{1, \ldots, M\} \times \mathbb{N} / J_m(ka_p) = 0\}$ and thus, following (1), $k \in F_D(\Omega)$ if and only if $\widetilde{\mathbb{L}}^{p,p}_{m,m} = 0$ for some $p = 1, \ldots, M$ and $m \in \mathbb{N}$ (recall that

$H_m^{(1)}(x) \neq 0\ \forall x \in \mathbb{R}$). For the finite dimensional approximation, we keep only $2N_p+1$ modes per obstacle Ω_p, $p=1,\ldots,M$, such that $-N_p \leq m \leq N_p$. The resulting truncated matrix $\mathbb{L}$ is then

$$\mathbb{L} = \begin{pmatrix} \mathbb{L}^{1,1} & \mathbb{L}^{1,2} & \ldots & \mathbb{L}^{1,M} \\ \mathbb{L}^{2,1} & \mathbb{L}^{2,2} & \ldots & \mathbb{L}^{2,1} \\ \vdots & \vdots & \ddots & \vdots \\ \mathbb{L}^{M,1} & \mathbb{L}^{M,2} & \ldots & \mathbb{L}^{M,M} \end{pmatrix},$$

where each $(2N_p+1)\times(2N_q+1)$ block $\mathbb{L}^{p,q}$ has for coefficient: $\mathbb{L}^{p,q}_{m,n} := \widetilde{\mathbb{L}}^{p,q}_{m,n}$, for $-N_p \leq m \leq N_p$ and $-N_q \leq n \leq N_q$.

3 Low frequency condition number estimates of the single-layer potential for close obstacles: the case of circular cylinders

In this Section, we assume that we have a dense media: the obstacles are *small* and *close*. In other words, setting $a = \min_{p=1,\ldots,M} a_p$ and $b = \min_{p,q=1,\ldots,M, p\neq q} b_{pq}$, we consider that both ka and kb tend towards 0 at the same speed. To analyze this regime, we potentially have two methods. The first one consists in choosing a fixed wave number k and applying a dilation to the geometrical configuration. The second one (that we follow here) is to fix the geometry and to let k tends towards 0. As a result, the radii a_p, the centers of the obstacles $\mathbf{O}_p$ as well as the distances between the centers b_{pq} are supposed to be constant. Following [6], we consider the limit matrix approach when k tends towards zero to derive some estimates of the eigenvalues μ_{min} and μ_{max} of the matrix $\mathbb{L}$, respectively with smallest and largest modulus. In particular, we show that μ_{min} can still be approximated by the eigenvalue with smallest modulus related to single scattering. As a by-product, these approximations allow us to derive condition number estimates.

3.1 The limit matrix approach

We extend the approach introduced in [6] to distant obstacles. We develop an asymptotic analysis of the coefficients of $\mathbb{L}$ when k tends towards 0. By using these approximations, we build a limit matrix $\mathbb{L}^0$ such that: $\mathbb{L} = \mathbb{L}^0 + O\left(k^2\ln(k)\right)$ and approximate the spectrum of $\mathbb{L}$ by the one of $\mathbb{L}^0$.

Let us recall that each diagonal block $\mathbb{L}^{p,p}$, for $p=1,\ldots,M$, is a diagonal matrix with coefficients $\mathbb{L}^{p,p}_{m,m}$

$$\mathbb{L}^{p,p}_{m,m} = \frac{i\pi a_p}{2} J_m(ka_p) H_m^{(1)}(ka_p), \qquad \text{for } m=-N_p,\ldots,N_p.$$

To simplify, let $I := \{(p,m)\in\mathbb{Z} \text{ such that } 1\leq p\leq M \text{ and } -N_p \leq m \leq N_p\}$ be the set of every indices p and m. From Lemma 1 in [6], we have the following result.

Lemma 1. *When $k\to 0$ and for every $(p,m)\in I$, the following result holds*

$$\mathbb{L}^{p,p}_{m,m} = \begin{cases} (\mathbb{L}^0)^{p,p}_{0,0} + O\left((k)^2\ln(k)\right) & \text{for } m=0, \\ (\mathbb{L}^0)^{p,p}_{m,m} + O\left((k)^2\right) & \text{for } m\neq 0, \end{cases} \tag{2}$$

setting

$$(\mathbb{L}^0)^{p,p}_{m,m} = \begin{cases} -a_p \left[\ln\left(\dfrac{k a_p}{2}\right) + \gamma \right] + i\dfrac{\pi a_p}{2} & \text{for } m = 0, \\ \dfrac{a_p}{2|m|} & \text{for } m \neq 0, \end{cases} \tag{3}$$

where $\gamma = 0.5772\ldots$ *is the Euler constant.*

Following [6], for $p = 1, \ldots, M$, we build the diagonal matrix $(\mathbb{L}^0)^{p,p}$, of size $(2N_p+1)\times(2N_p+1)$, defined by

$$(\mathbb{L}^0)^{p,p} = \begin{pmatrix} (\mathbb{L}^0)^{p,p}_{-N_p,-N_p} & 0 & 0 & \ldots & 0 \\ 0 & \ddots & \ddots & & 0 \\ \vdots & \ddots & (\mathbb{L}^0)^{p,p}_{0,0} & \ddots & \vdots \\ 0 & & \ddots & \ddots & 0 \\ 0 & \ldots & 0 & 0 & (\mathbb{L}^0)^{p,p}_{N_p,N_p} \end{pmatrix}, \tag{4}$$

where the coefficients $(\mathbb{L}^0)^{p,p}_{m,m}$ are given by Eq. (3). When $k \to 0$, relation (2) implies that $\mathbb{L}^{p,p} = (\mathbb{L}^0)^{p,p} + O\left(k^2 \ln(k)\right)$, for $p = 1, \ldots, M$. Let us remark that the limit matrix $(\mathbb{L}^0)^{p,p}$ is the same as for distant obstacles. This is expected since the difference lies in the parameters kb_{pq} (b_{pq} is the distance between Ω_p and Ω_q) which only appears in the off-diagonal blocks $\mathbb{L}^{p,q}$, for $p \neq q$.

The asymptotic behaviors of the off-diagonal blocks coefficients $\mathbb{L}^{p,q}_{m,n}$ differ according to the indices m and n. We split each block $\mathbb{L}^{p,q}$, for $p \neq q$, into 5 zones, labeled from 0 to 4, as reported on Figure 1. We next develop an asymptotic analysis of the coefficients $\mathbb{L}^{p,q}_{m,n}$ when $k \to 0$ with respect to each zone. The results are summarized in the following Lemma.

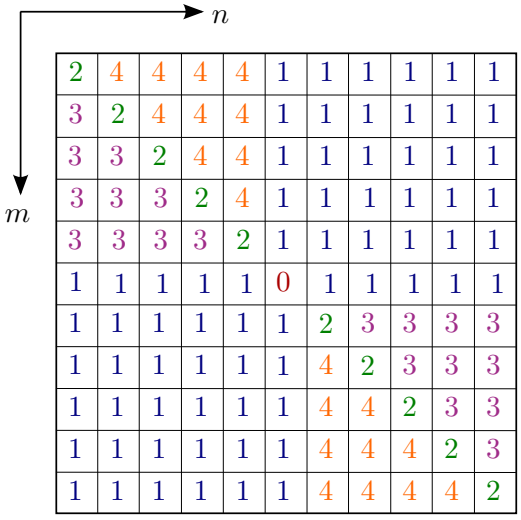

Figure 1: Decomposition of $\mathbb{L}^{p,q}$ into five different zones, for $p \neq q$.

Lemma 2. *Let* $(p, m) \in I$ *and* $(q, n) \in I$, *with* $p \neq q$. *When* k *tends towards* 0, *the coefficients* $\mathbb{L}^{p,q}_{m,n}$ *of the matrix* $\mathbb{L}$ *have the following asymptotic behavior*

• ***Zone*** 0*:* $(m = n = 0)$

$$\mathbb{L}_{0,0}^{p,q} = -\sqrt{a_p a_q}\left[\ln\left(\frac{kb_{pq}}{2}\right) + \gamma\right] + i\frac{\pi\sqrt{a_p a_q}}{2} + O\left(k^2\ln(k)\right).$$

• ***Zone*** 1*:* $(mn \leq 0 \ \textit{and}\ (m,n) \neq (0,0))$

$$\mathbb{L}_{m,n}^{p,q} = \begin{cases} i(-1)^m \dfrac{\sqrt{a_p a_q}}{2} \dfrac{1}{|m|!|n|!}\left(\dfrac{a_p}{b_{pq}}\right)^{|m|}\left(\dfrac{a_q}{b_{pq}}\right)^{|n|} e^{i(n-m)\alpha_{pq}} + O\left(k^2\ln(k)\right) & \textit{if } |m|+|n|=1, \\ i(-1)^m \dfrac{\sqrt{a_p a_q}}{2} \dfrac{(|m|+|n|-1)!}{|m|!|n|!}\left(\dfrac{a_p}{b_{pq}}\right)^{|m|}\left(\dfrac{a_q}{b_{pq}}\right)^{|n|} e^{i(n-m)\alpha_{pq}} + O\left(k^2\right) & \textit{otherwise.} \end{cases}$$

• ***Zone*** 2*:* $(n = m, m \neq 0 \ \textit{and}\ n \neq 0)$

$$\mathbb{L}_{m,m}^{p,q} = O\left(k^{2|m|}\ln(k)\right).$$

• ***Zone*** 3*:* $((0 > m > n) \ \textit{or}\ (0 < m < n))$

$$\mathbb{L}_{m,n}^{p,q} = O\left(k^{2|m|}\right).$$

• ***Zone*** 4*:* $((0 > n > m) \ \textit{or}\ (0 < n < m))$

$$\mathbb{L}_{m,n}^{p,q} = O\left(k^{2|n|}\right).$$

Proof. We prove the results zone by zone.

• **Zone** 0, $m = n = 0$. In this zone, the coefficients $\mathbb{L}_{m,n}^{p,q}$ write down

$$\mathbb{L}_{0,0}^{p,q} = i\frac{\pi\sqrt{a_p a_q}}{2} J_0(ka_p) H_0^{(1)}(kb_{pq}) J_0(ka_q). \tag{5}$$

Let us recall that, when $k \to 0$, the first kind Hankel's function of order zero has the following expansion (see relations (9.1.8) and (9.1.13) in [1])

$$H_0^{(1)}(kb_{pq}) = 1 + i\frac{2}{\pi}\left[\ln\left(\frac{kb_{pq}}{2}\right) + \gamma\right] + O\left(k^2\ln(k)\right), \tag{6}$$

and the Bessel's function of order $m \in \mathbb{N}$ is such that (Eq. (9.1.10) in [1])

$$J_m(ka_p) = \frac{1}{m!}\left(\frac{ka_p}{2}\right)^m + O\left(k^{m+2}\right). \tag{7}$$

By injecting (7) and (6) into (5), we obtain

$$\mathbb{L}_{0,0}^{p,q} = i\frac{\pi\sqrt{a_p a_q}}{2}\left[1 + O\left(k^2\right)\right]\left[1 + i\frac{2}{\pi}\left[\ln\left(\frac{kb_{pq}}{2}\right) + \gamma\right] + O\left(k^2\ln(k)\right)\right]\left[1 + O\left(k^2\right)\right],$$

which leads to the expected relation

$$\mathbb{L}_{0,0}^{p,q} = -\sqrt{a_p a_q}\left[\ln\left(\frac{kb_{pq}}{2}\right) + \gamma\right] + i\frac{\pi\sqrt{a_p a_q}}{2} + O\left(k^2\ln(k)\right).$$

• **Zone** 1 ($mn \leq 0$ and $(m,n) \neq (0,0)$). Let us introduce the sign function, denoted by sgn, such that for any $n \in \mathbb{Z}$, $\mathrm{sgn}(n) = 1$ if $n \geq 0$ and $\mathrm{sgn}(n) = -1$ if $n < 0$. Using some properties of the special functions, we can write the coefficients $\mathbb{L}_{m,n}^{p,q}$ under the following form

$$\mathbb{L}_{m,n}^{p,q} = (\mathrm{sgn}(m))^m (\mathrm{sgn}(n))^n (\mathrm{sgn}(n-m))^{n-m} i \frac{\pi\sqrt{a_p a_q}}{2} e^{i(n-m)\alpha_{pq}} J_{|m|}(ka_p) H^{(1)}_{|n-m|}(kb_{pq}) J_{|n|}(ka_q). \tag{8}$$

Let us note that the indices of the Bessel's and Hankel's functions are now positive. For the coefficients of zone 1, the indices m and n satisfy $mn \leq 0$. Since $|n-m| = |n| + |m|$, $\mathrm{sgn}(m) = -\mathrm{sgn}(n)$ and $\mathrm{sgn}(n-m) = \mathrm{sgn}(n)$, we have

$$(\mathrm{sgn}(m))^m (\mathrm{sgn}(n))^n (\mathrm{sgn}(n-m))^{n-m} = (-\mathrm{sgn}(n))^m (\mathrm{sgn}(n))^n (\mathrm{sgn}(n))^{n+m} = (-1)^m.$$

By using (8), the coefficients $\mathbb{L}_{m,n}^{p,q}$ in this zone can be written

$$\mathbb{L}_{m,n}^{p,q} = (-1)^m i \frac{\pi\sqrt{a_p a_q}}{2} e^{i(n-m)\alpha_{pq}} J_{|m|}(ka_p) H^{(1)}_{|m|+|n|}(kb_{pq}) J_{|n|}(ka_q). \tag{9}$$

Let us recall the asymptotic expansions of the first kind Hankel's functions of order $m > 0$ when $k \to 0$ (see relations (9.1.9) and (9.1.11) in [1])

$$H_m^{(1)}(kb_{pq}) = \frac{(m-1)!}{\pi} \left(\frac{kb_{pq}}{2}\right)^{-m} + O\left(f_m(k)\right), \tag{10}$$

where the functions f_m are defined by: $f_1(k) = k\ln(k)$ and $f_m(k) = k^{2-m}$ for $m \geq 2$. Next, we use the expansions (7) and (10) of the Bessel's and Hankel's functions into the expression (9) to get

$$\mathbb{L}_{m,n}^{p,q} = i(-1)^m \frac{\pi\sqrt{a_p a_q}}{2} e^{i(n-m)\alpha_{pq}} \left[\frac{1}{|m|!}\left(\frac{ka_p}{2}\right)^{|m|} + O\left(k^{|m|+2}\right)\right] \left[\frac{(|m|+|n|-1)!}{\pi}\left(\frac{kb_{pq}}{2}\right)^{-|m|-|n|} + O\left(f_{|m|+|n|}(k)\right)\right] \left[\frac{1}{|n|!}\left(\frac{ka_q}{2}\right)^{|n|} + O\left(k^{|n|+2}\right)\right].$$

Let us note that we can use the asymptotic relation (10) of the Hankel's functions of order $|m|+|n|$. Indeed, for the coefficients in this zone, the indices (m,n) satisfy $mn \leq 0$ and $(m,n) \neq (0,0)$, which in particular implies that $|m|+|n| \neq 0$. Hence we study the Hankel's functions with non null index. We then develop the previous relation to obtain

$$\mathbb{L}_{m,n}^{p,q} = i(-1)^m \frac{\sqrt{a_p a_q}}{2} e^{i(n-m)\alpha_{pq}} \frac{(|m|+|n|-1)!}{|m|!|n|!}\left(\frac{ka_p}{2}\right)^{|m|}\left(\frac{ka_q}{2}\right)^{|n|}\left(\frac{2}{kb_{pq}}\right)^{|m|+|n|} + O\left(k^{|n|+|m|+2-|m|-|n|}\right) + O\left(k^{|m|+|n|} f_{|m|+|n|}(k)\right).$$

After some simplifications, we have

$$\mathbb{L}_{m,n}^{p,q} = i(-1)^m \frac{\sqrt{a_p a_q}}{2} \frac{(|m|+|n|-1)!}{|m|!|n|!}\left(\frac{a_p}{b_{pq}}\right)^{|m|}\left(\frac{a_q}{b_{pq}}\right)^{|n|} e^{i(n-m)\alpha_{pq}} + O\left(k^2\right) + O\left(k^{|m|+|n|} f_{|m|+|n|}(k)\right). \tag{11}$$

From the definition of the functions $f_{|m|+|n|}$, we have

$$k^{|m|+|n|} f_{|m|+|n|}(k) = \begin{cases} k^2 \ln(k) & \text{if } |m|+|n| = 1, \\ k^2 & \text{otherwise.} \end{cases}$$

By injecting these relations into (11), we obtain the expected relation.

• **Zone** 2, ($n = m, m \neq 0$ and $n \neq 0$). To prove the relations in the zones 2, 3 and 4, we only need to analyze the modulus of the coefficient $\mathbb{L}^{p,q}_{m,n}$

$$\left|\mathbb{L}^{p,q}_{m,n}\right| = \frac{\sqrt{a_p a_q}}{2} \left|J_{|m|}(ka_p)\right| \left|H^{(1)}_{|n-m|}(kb_{pq})\right| \left|J_{|n|}(ka_q)\right|. \tag{12}$$

For zone 2, we have $|n-m| = 0$, with $m \neq 0$ and $n \neq 0$ and then

$$\left|\mathbb{L}^{p,q}_{m,n}\right| = \frac{\sqrt{a_p a_q}}{2} \left|J_{|m|}(ka_p)\right| \left|H^{(1)}_{0}(kb_{pq})\right| \left|J_{|n|}(ka_q)\right|.$$

By using the asymptotics (7) and (6) we obtain

$$\left|\mathbb{L}^{p,q}_{m,n}\right| = \left| \frac{\pi\sqrt{a_p a_q}}{2} \left[\left(\frac{ka_p}{2}\right)^{|m|} + O\left(k^{|m|+2}\right)\right] \left[1 + i\frac{2}{\pi}\left[\ln\left(\frac{kb_{pq}}{2}\right) + \gamma\right] + O\left(k^2\ln(k)\right)\right] \left[\left(\frac{ka_q}{2}\right)^{|m|} + O\left(k^{|m|+2}\right)\right] \right|.$$

This directly proves that $\mathbb{L}^{p,q}_{m,n} = O\left(k^{2|m|}\ln(k)\right)$.

• **Zone** 3: since $(0 > m > n)$ or $(0 < m < n)$, we have $|n-m| = |n| - |m|$ and

$$\left|\mathbb{L}^{p,q}_{m,n}\right| = \frac{\sqrt{a_p a_q}}{2} \left|J_{|m|}(ka_p)\right| \left|H^{(1)}_{|n|-|m|}(kb_{pq})\right| \left|J_{|n|}(ka_q)\right|.$$

By using (7) and (10) one gets

$$\left|\mathbb{L}^{p,q}_{m,n}\right| = \left| \frac{\pi\sqrt{a_p a_q}}{2} \left[\frac{1}{|m|!}\left(\frac{ka_p}{2}\right)^{|m|} + O\left(k^{|m|+2}\right)\right] \left[\frac{(|n|-|m|-1)!}{\pi}\left(\frac{kb_{pq}}{2}\right)^{-|n|+|m|} + O\left(f_{|n|-|m|}(k)\right)\right] \left[\frac{1}{|n|!}\left(\frac{ka_q}{2}\right)^{|n|} + O\left(k^{|n|+2}\right)\right] \right|$$

and obtain: $\mathbb{L}^{p,q}_{m,n} = O\left(k^{2|m|}\right)$.

• **Zone** 4: since $(0 > n > m)$ or $(0 < n < m)$, we have: $|n-m| = |m| - |n|$. Let us point out that, by changing the role of m and n, we recover the results of zone 3. Thus, the proof developed above can be adapted here to directly obtain $\mathbb{L}^{p,q}_{m,n} = O\left(k^{2|n|}\right)$. □

For any $1 \leq p \neq q \leq M$, let us introduce the limit matrix $(\mathbb{L}^0)^{p,q}$ with coefficients

$$(\mathbb{L}^0)^{p,q}_{m,n} = \begin{cases} -\sqrt{a_p a_q}\left[\ln\left(\frac{kb_{pq}}{2}\right) + \gamma\right] + i\frac{\pi\sqrt{a_p a_q}}{2} & \text{if } (m,n) = (0,0), \\ (-1)^m \frac{i\sqrt{a_p a_q}}{2} \frac{(|m|+|n|-1)!}{|m|!|n|!} \left(\frac{a_p}{b_{pq}}\right)^{|m|} \left(\frac{a_q}{b_{pq}}\right)^{|n|} e^{i(n-m)\alpha_{pq}} & \text{if } (m,n) \neq (0,0) \text{ and } mn \leq 0, \\ 0 & \text{otherwise,} \end{cases} \tag{13}$$

for $-N_p \leq m \leq N_p$ and $-N_q \leq n \leq N_q$, Moreover, from Lemma 2, we have the following relation

$$\mathbb{L}^{p,q} = (\mathbb{L}^0)^{p,q} + O\left(k^2 \ln(k)\right), \qquad \text{for } p \neq q. \tag{14}$$

Let us now introduce the block matrix $\mathbb{L}^0$ containing each submatrix $(\mathbb{L}^0)^{p,q}$ and defined by

$$\mathbb{L}^0 = \begin{pmatrix} (\mathbb{L}^0)^{1,1} & (\mathbb{L}^0)^{1,2} & \dots & (\mathbb{L}^0)^{1,M} \\ (\mathbb{L}^0)^{2,1} & (\mathbb{L}^0)^{2,2} & \dots & (\mathbb{L}^0)^{2,1} \\ \vdots & \vdots & \ddots & \vdots \\ (\mathbb{L}^0)^{M,1} & (\mathbb{L}^0)^{M,2} & \dots & (\mathbb{L}^0)^{M,M} \end{pmatrix}.$$

By using (4) and (14), the following proposition holds.

Proposition 1. *When k tends towards zero, the truncated matrix $\mathbb{L}$ of the single-layer operator L satisfies the relation*

$$\mathbb{L} = \mathbb{L}^0 + O\left(k^2 \ln(k)\right). \tag{15}$$

To visualize the relatively sparse structure of $\mathbb{L}^0$, we represent on Figure 2 in grey color the non zero coefficients (skeleton of $\mathbb{L}^0$) in the case of two circular scatterers.

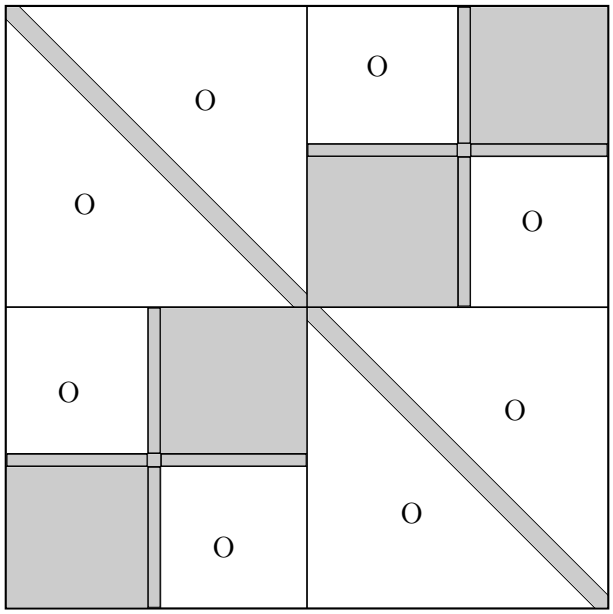

Figure 2: Non null coefficients of the matrix $\mathbb{L}^0$ for a configuration with two obstacles. The grey zones correspond to the non zero coefficients.

From now on, let us respectively denote by $(\mu_m^p)_{(p,m)\in I}$ and $((\mu^0)_m^p)_{(p,m)\in I}$ the eigenvalues of $\mathbb{L}$ and $\mathbb{L}^0$. For $(p,m) \in I$, we moreover assume that

$$\mu_m^p \simeq (\mu^0)_m^p, \tag{16}$$

which is coherent with (15). To motivate our approach, we compare the eigenvalues of $\mathbb{L}$ and $\mathbb{L}^0$ on Figures 3(b)-3(d), for $k = 0.1$ and 30 randomly distributed disks of radius 0.1 in $[0,4]^2$

(see the example of Figure 3(a)). For $p, q = 1, \ldots, M$, with $p \neq q$, $N_p = 5$ and the intercenter distance b_{pq} is such that: $0.33 \leq b_{pq} \leq 4.59$. The eigenvalues are computed by the Matlab function `eig`. We observe that the approximation of the eigenvalues $(\mu_m^p)_{(p,m)\in I}$ of $\mathbb{L}$ by the eigenvalues $((\mu^0)_m^p)_{(p,m)\in I}$ of $\mathbb{L}^0$ is satisfactory. Let us denote by μ_{max} and μ_{max}^0 the eigenvalues with largest modulus of respectively $\mathbb{L}$ and $\mathbb{L}^0$. On Figure 3(b), we observe that they are very close which is numerically confirmed since: $\mu_{max} \simeq 5.393 + 4.623i$ and $\mu_{max}^0 \simeq 5.494 + 4.695i$. This implies that: $|\mu_{max}| \simeq 7.103$ and $|\mu_{max}^0| \simeq 7.227$. Furthermore, the eigenvalues with smallest modulus of $\mathbb{L}$ and $\mathbb{L}^0$, respectively denoted by μ_{min} and μ_{min}^0, are also very close (see Figure 3(d)). The numerical values confirm this result: $\mu_{min} \simeq 0.01 + 10^{-13}i$, and $\mu_{min}^0 \simeq 0.01 + 10^{-13}i$.

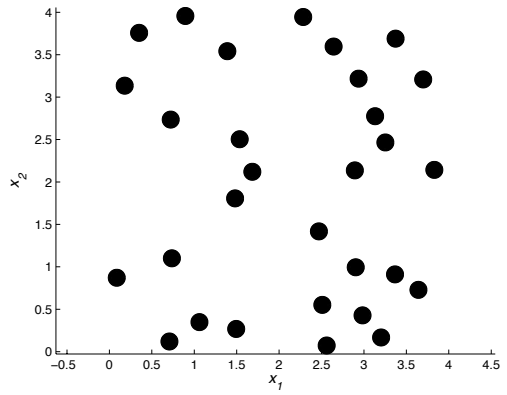

(a) Obstacles positions

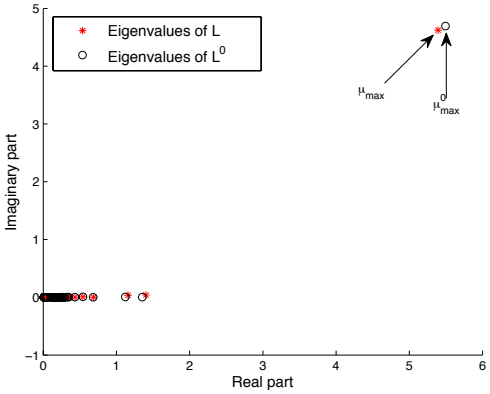

(b) Eigenvalues of $\mathbb{L}$ and $\mathbb{L}^0$

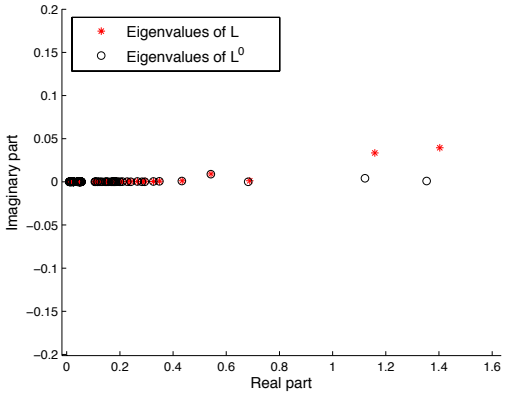

(c) Zoom of Figure (b) around the origin

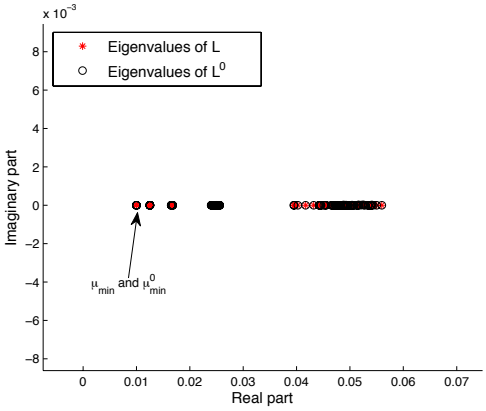

(d) Zoom around the eigenvalues with smallest modulus μ_{min} and μ_{min}^0

Figure 3: Comparison of the eigenvalues of $\mathbb{L}$ and $\mathbb{L}^0$ for 30 randomly and identical distributed disks of radius $a_p = 0.1$ in $[0, 4]^2$, $N_p = 5$ for each obstacle ($k = 0.1$ and $0.33 \leq b_{pq} \leq 4.59$).

This example confirms that our approach seems reasonable. Further simulations have been performed and show that the eigenvalues of $\mathbb{L}^0$ are close to the ones associated with $\mathbb{L}$. To simplify the computations, we assume that, for any $p = 1, \ldots, M$, we have: $a_p = a$ and $N_p = N$. Let us recall that, with these assumptions, for $p = 1, \ldots, M$, the diagonal blocks $(\mathbb{L}^0)^{p,p}$ are independent

of p. Moreover, we have $(\mathbb{L}^0)^{p,p}_{m,m} = (\mathbb{L}^0)^{p,p}_{-m,-m} = (\mathbb{L}^0)^{q,q}_{m,m} = (\mathbb{L}^0)^{q,q}_{-m,-m}$, for $(p,m) \in I$ and $q = 1, \ldots, M$. These terms are now denoted by $\widehat{\mathbb{L}}_m$

$$\forall p = 1, \ldots, M,\ \forall m = 0, \ldots, N, \qquad \widehat{\mathbb{L}}_m = (\mathbb{L}^0)^{p,p}_{m,m} = \begin{cases} -a\left[\ln\left(\dfrac{ka}{2}\right) + \gamma\right] + i\dfrac{\pi a}{2}, & \text{if } m = 0, \\ \dfrac{a}{2m}, & \text{otherwise.} \end{cases}$$

3.2 Estimates of the eigenvalue with smallest modulus

Let us now estimate the eigenvalue with smallest modulus μ^0_{min} of $\mathbb{L}^0$. Like for the case of distant obstacles [6], an approach based on the Gershgorin-Hadamard discs has been developed but provides inaccurate estimates of the eigenvalue with smallest modulus. In addition, the obtained approximation for the largest eigenvalue is not precise, most particularly for many obstacles.

Like in [6], we show that the eigenvalue of $\mathbb{L}^0$ (and next $\mathbb{L}$) with smallest modulus can be approximated correctly by the associated single scattering eigenvalue: $\widehat{\mathbb{L}}_N = a/(2N)$, with multiplicity $2M$. To prove this result, we build an approximate eigenvector of $\mathbb{L}^0$ for the approximate eigenvalue $\widehat{\mathbb{L}}_{|m|}$, for large $|m|$. Let us introduce the vector $\mathbf{X}^{(p,m)}$, for $(p,m) \in I$, given by

$$\mathbf{X}^{(p,m)} = \begin{pmatrix} \mathbf{X}^{(p,m)}_1 \\ \mathbf{X}^{(p,m)}_2 \\ \vdots \\ \mathbf{X}^{(p,m)}_M \end{pmatrix}.$$

Each block $\mathbf{X}^{(p,m)}_q = (X^{(p,m)}_{q,n})_{n=-N,\ldots,N}$, for $q = 1, \ldots, M$, has size $2N+1$ and its components are defined by the following relations

$$X^{(p,m)}_{p,n} = \begin{cases} 1 & \text{if } n = m, \\ 0 & \text{otherwise,} \end{cases} \qquad \text{for } q = p, \tag{17}$$

and

$$X^{(p,m)}_{q,n} = 0, \qquad \text{for } q \neq p. \tag{18}$$

Hence, the blocks $\mathbf{X}^{(p,m)}_q$ are zero for $q \neq p$, and $\mathbf{X}^{(p,m)}_p = (X^{(p,m)}_{p,n})_{n=-N,\ldots,N}$ has only one nonzero component localized at $n = m$ (and equal to 1). Let us remark that $\mathbf{X}^{(p,m)}$ is also normalized for both the infinity and euclidian norms. We introduce now $\mathbf{Y}^{(p,m)}$ as the vector resulting from the matrix-vector product between $\mathbb{L}^0$ and $\mathbf{X}^{(p,m)}$

$$\mathbf{Y}^{(p,m)} = \mathbb{L}^0\mathbf{X}^{(p,m)} = \begin{pmatrix} \mathbf{Y}^{(p,m)}_1 \\ \mathbf{Y}^{(p,m)}_2 \\ \vdots \\ \mathbf{Y}^{(p,m)}_M \end{pmatrix} = \begin{pmatrix} (\mathbb{L}^0)^{1,p}\mathbf{X}^{(p,m)}_p \\ (\mathbb{L}^0)^{2,p}\mathbf{X}^{(p,m)}_p \\ \vdots \\ (\mathbb{L}^0)^{M,p}\mathbf{X}^{(p,m)}_p \end{pmatrix}.$$

Let us focus on the vectorial block $\mathbf{Y}^{(p,m)}_p$. From (4), we have

$$Y^{(p,m)}_{p,n} = \begin{cases} (\mathbb{L}^0)^{p,p}_{m,m} = \widehat{\mathbb{L}}_{|m|} & \text{if } n = m, \\ 0 & \text{otherwise.} \end{cases}$$

Moreover, relation (17) implies that $\mathbf{Y}_p^{(p,m)} = \widehat{\mathbb{L}}_{|m|}\mathbf{X}_p^{(p,m)}$. Let us now analyze the vectors $\mathbf{Y}_q^{(p,m)} = (\mathbb{L}^0)^{q,p}\mathbf{X}_p^{(p,m)}$, for $q = 1, \dots, M$ and $q \neq p$. By using the particular structure of $\mathbf{X}_p^{(p,m)}$ (see (17)), the coefficients $Y_{q,n}^{(p,m)}$ satisfy

$$Y_{q,n}^{(p,m)} = (\mathbb{L}^0)_{n,m}^{q,p}, \qquad \text{for } -N \leq n \leq N.$$

If $\|\cdot\|_2$ denotes the usual 2-norm, we then have the following equality

$$\left\| \mathbb{L}^0\mathbf{X}^{(p,m)} - \widehat{\mathbb{L}}_{|m|}\mathbf{X}^{(p,m)} \right\|_2^2 = \sum_{\substack{q=1 \\ q\neq p}}^{M} \sum_{n=-N}^{N} \left| (\mathbb{L}^0)_{m,n}^{p,q} \right|^2. \tag{19}$$

Our goal is to prove that $\mathbf{X}^{(p,m)}$ is an approximate eigenvector of $\mathbb{L}^0$, with approximate eigenvalue $\widehat{\mathbb{L}}_{|m|}$, for $|m|$ sufficiently large. To this end, we need to find an upper bound for

$$\left\| \mathbb{L}^0\mathbf{X}^{(p,m)} - \widehat{\mathbb{L}}_{|m|}\mathbf{X}^{(p,m)} \right\|_2^2.$$

Indeed, this term measures the error related to the approximation of an eigenvector of $\mathbb{L}^0$ by $\mathbf{X}^{(p,m)}$ with approximate eigenvalue $\widehat{\mathbb{L}}_{|m|}$. We first have

$$\left\| \mathbb{L}^0\mathbf{X}^{(p,m)} - \widehat{\mathbb{L}}_{|m|}\mathbf{X}^{(p,m)} \right\|_2^2 \leq \left(\sum_{\substack{q=1 \\ q\neq p}}^{M} \sum_{n=-N}^{N} \left| (\mathbb{L}^0)_{m,n}^{p,q} \right| \right)^2. \tag{20}$$

Let us now state the following Lemma.

Lemma 3. *Let $(p,m) \in I$ and $q = 1, \dots, M$, such that $p \neq q$ and $m \neq 0$. The following inequality holds*

$$\sum_{n=-N}^{N} \left| (\mathbb{L}^0)_{n,m}^{q,p} \right| \leq \frac{a}{2|m|} \left(\frac{a}{b_{pq} - a} \right)^{|m|}. \tag{21}$$

Proof. Let us consider three integers $p, q = 1, \dots, M$ and $m = -N, \dots, N$ such that $p \neq q$ and $m \neq 0$. From definition (13) of the coefficients $(\mathbb{L}^0)_{m,n}^{p,q}$, we have

$$\sum_{n=-N}^{N} \left| (\mathbb{L}^0)_{n,m}^{q,p} \right| = \frac{a}{2} \left(\frac{a}{b_{pq}} \right)^{|m|} \sum_{n=0}^{N} \frac{(|m| + |n| - 1)!}{|m|!|n|!} \left(\frac{a}{b_{pq}} \right)^{|n|}.$$

Since $|m|! = |m|(|m-1|!)$, we can write

$$\sum_{n=-N}^{N} \left| (\mathbb{L}^0)_{n,m}^{q,p} \right| = \frac{a}{2|m|} \left(\frac{a}{b_{pq}} \right)^{|m|} \sum_{n=0}^{N} \frac{(|m| + |n| - 1)!}{(|m|-1)!|n|!} \left(\frac{a}{b_{pq}} \right)^{|n|}.$$

Then one gets

$$\sum_{n=-N}^{N} \left| (\mathbb{L}^0)_{n,m}^{q,p} \right| = \frac{a}{2|m|} \left(\frac{a}{b_{pq}} \right)^{|m|} \sum_{n=0}^{N} \binom{|m| + |n| - 1}{|m| - 1} \left(\frac{a}{b_{pq}} \right)^{|n|}, \tag{22}$$

where

$$\binom{|m|+|n|-1}{|m|-1} = \frac{(|m|+|n|-1)!}{(|m|-1)!|n|!}.$$

Since $a < b_{pq}$, the series indexed by n appearing in the right-hand side of the equality (22) is converging when N tends towards infinity. More precisely, we have

$$\lim_{N\to\infty} \sum_{n=0}^{N} \binom{|m|+|n|-1}{|m|-1} \left(\frac{a}{b_{pq}}\right)^{|n|} = \left(1-\frac{a}{b_{pq}}\right)^{-|m|} = \left(\frac{b_{pq}}{b_{pq}-a}\right)^{|m|}.$$

Furthermore, since each term of the series is positive, the following inequality is fulfilled for any $N \in \mathbb{N}$

$$\sum_{n=0}^{N} \binom{|m|+|n|-1}{|m|-1} \left(\frac{a}{b_{pq}}\right)^{|n|} \leq \left(\frac{b_{pq}}{b_{pq}-a}\right)^{|m|}.$$

By using the upper bound in (22), we finally obtain

$$\sum_{n=-N}^{N} \left|(\mathbb{L}^0)^{q,p}_{n,m}\right| \leq \frac{a}{2|m|} \left(\frac{a}{b_{pq}-a}\right)^{|m|}.$$

□

This Lemma leads to a fine upper bound of the euclidian norm

$$\left\| \mathbb{L}^0 \mathbf{X}^{(p,m)} - \widehat{\mathbb{L}}_{|m|} \mathbf{X}^{(p,m)} \right\|_2,$$

and shows that $\mathbf{X}^{(p,m)}$ can be used as an approximate eigenvector of $\mathbb{L}^0$. We summarize these results in the following proposition.

Proposition 2. *Let $(p,m) \in I$ with $m \neq 0$. The vector $\mathbf{X}^{(p,m)}$ defined by relations (17) and (18) is an approximate eigenvector of $\mathbb{L}^0$ with approximate eigenvalue $\widehat{\mathbb{L}}_{|m|}$, in the sense that the relative error between $\mathbb{L}^0\mathbf{X}^{(p,m)}$ and $\widehat{\mathbb{L}}_{|m|}\mathbf{X}^{(p,m)}$ satisfies the following upper bound*

$$\frac{\left\| \mathbb{L}^0 \mathbf{X}^{(p,m)} - \widehat{\mathbb{L}}_{|m|} \mathbf{X}^{(p,m)} \right\|_2}{\widehat{\mathbb{L}}_{|m|}} \leq \sum_{\substack{q=1 \\ q\neq p}}^{M} \left(\frac{a}{b_{pq}-a}\right)^{|m|}. \tag{23}$$

Proof. By applying Lemma 3 to the first inequality (20) for $\left\| \mathbb{L}^0 \mathbf{X}^{(p,m)} - \widehat{\mathbb{L}}_{|m|} \mathbf{X}^{(p,m)} \right\|_2$ we obtain

$$\left\| \mathbb{L}^0 \mathbf{X}^{(p,m)} - \widehat{\mathbb{L}}_{|m|} \mathbf{X}^{(p,m)} \right\|_2^2 \leq \left(\sum_{\substack{q=1 \\ q\neq p}}^{M} \frac{a}{2|m|} \left(\frac{a}{b_{pq}-a}\right)^{|m|} \right)^2.$$

Since all the terms with index q appearing in the sum are positive, we can take the square-root of the inequality to get

$$\left\| \mathbb{L}^0 \mathbf{X}^{(p,m)} - \widehat{\mathbb{L}}_{|m|} \mathbf{X}^{(p,m)} \right\|_2 \leq \frac{a}{2|m|} \sum_{\substack{q=1 \\ q\neq p}}^{M} \left(\frac{a}{b_{pq}-a}\right)^{|m|}.$$

Finally, we use $\widehat{\mathbb{L}}_{|m|} = \dfrac{a}{2|m|}$ and obtain

$$\frac{\left\| \mathbb{L}^0 \mathbf{X}^{(p,m)} - \widehat{\mathbb{L}}_{|m|} \mathbf{X}^{(p,m)} \right\|_2}{\widehat{\mathbb{L}}_{|m|}} \leq \sum_{\substack{q=1 \\ q \neq p}}^{M} \left(\frac{a}{b_{pq} - a} \right)^{|m|}.$$

□

For $(p,m) \in I$ with $m \neq 0$ and $|m|$ sufficiently large, this proposition shows that $\mathbf{X}^{(p,m)}$ is an approximate eigenvector of $\mathbb{L}^0$ with approximate eigenvalue $\widehat{\mathbb{L}}_{|m|}$. Moreover, the $2M$ vectors $(\mathbf{X}^{(p,m)})_{p=1,\ldots,M}$ and $(\mathbf{X}^{(p,-m)})_{p=1,\ldots,M}$ are approximate eigenvectors associated with the same approximate eigenvalue $\widehat{\mathbb{L}}_{|m|}$. Hence, for $|m|$ large enough, the quantity $\widehat{\mathbb{L}}_{|m|}$ is an approximate eigenvalue of $\mathbb{L}^0$ with multiplicity $2M$. The sequence $(\widehat{\mathbb{L}}_m)_{m\geq 1} = (\frac{a}{2m})_{m\geq 1}$ decays and tends towards 0 when m tends to infinity. The term $\widehat{\mathbb{L}}_N$ is then the smallest approximate eigenvalue $(\widehat{\mathbb{L}}_m)_{m\geq 1}$. Furthermore, $\widehat{\mathbb{L}}_N$ tends to 0 when N tends to infinity. This is the reason why we estimate μ^0_{min}, and next μ_{min}, by $\widehat{\mathbb{L}}_N$ with a multiplicity equal to $2M$, that is

$$\mu_{min} \simeq \mu^0_{min} \simeq \widehat{\mathbb{L}}_N. \tag{24}$$

Let us remark that $\widehat{\mathbb{L}}_N$ is also the approximation of the smallest eigenvalue in the framework of single scattering as well as multiple scattering for distant scatterers [6]. This approximation is more accurate as N is large and that the coupling between the obstacles is weak, that is when the obstacles are not too close. Indeed, the larger the distance b_{pq} is, the smaller the left hand side of the inequality (23) is. Similarly, the right hand side term of (23) (with $|m| = N$) is smaller as N is larger. Let us now come back to the example in Figure 3. The parameters were: 30 randomly distributed disks of radius 0.1 in $[0,4]^2$, $N = 5$, $k = 0.1$ and $0.33 \leq b_{pq} \leq 4.59$. The numerical computation of the smallest eigenvalues of $\mathbb{L}$ and $\mathbb{L}^0$ provide $\mu_{min} \simeq 0.01 + 10^{-13}i$ and $\mu^0_{min} \simeq 0.01 + 10^{-13}i$. Our estimate gives $\widehat{\mathbb{L}}_N = 0.01$, with a small relative error on μ_{min} equal to

$$100 \frac{\left| \mu_{min} - \widehat{\mathbb{L}}_N \right|}{|\mu_{min}|} \simeq 0.08\%.$$

3.3 Estimates of the eigenvalue with largest modulus

Unlike the previous case, we cannot construct an approximate eigenvector of $\mathbb{L}^0$ to provide an estimate of the largest eigenvalue μ^0_{max} of $\mathbb{L}^0$. By analyzing the expression (13) of the coefficients of the limit matrix $\mathbb{L}^0$, none of them depends on k, except the coefficients associated with the indices $m = n = 0$ which have a logarithmic growth with respect to k (*zone* 0 in Lemma 2). When the wavenumber k is small enough, the information related to the largest eigenvalue is *a priori* contained in these coefficients.

As in [6], we propose to extract the matrix $\mathbb{L}^1$ from $\mathbb{L}^0$ and related to the zero order modes. From relation (13), this $M \times M$ matrix $\mathbb{L}^1$ is defined, for $p, q = 1, \ldots, M$, by

$$(\mathbb{L}^1)^{p,q} = (\mathbb{L}^0)^{p,q}_{0,0} = \begin{cases} -a \left[\ln\left(\dfrac{ka}{2} \right) + \gamma \right] + i\dfrac{\pi a}{2}, & \text{if } p = q, \\ -a \left[\ln\left(\dfrac{kb_{pq}}{2} \right) + \gamma \right] + i\dfrac{\pi a}{2}, & \text{if } p \neq q. \end{cases} \tag{25}$$

Let us denote by μ^0_{max}, respectively μ^1_{max}, the eigenvalue with largest modulus of $\mathbb{L}^0$, respectively $\mathbb{L}^1$. We then estimate the largest eigenvalue of $\mathbb{L}^0$ by the one of $\mathbb{L}^1$, that is: $\mu^0_{max} \simeq \mu^1_{max}$. Next, from (16), we also estimate μ_{max} by μ^1_{max}. We compared three approaches to estimate μ^1_{max}. Two consist in bounding the spectral radius of $\mathbb{L}^1$, and so the modulus of μ^1_{max}, by computing the Frobenius norm of $\mathbb{L}^1$ or by applying the Gershgorin's discs theorem to $\mathbb{L}^1$. In both cases, the result was less accurate than for the third approach. Moreover, the expression of the estimate obtained by this last method is simpler. This is the reason why we only present this approach here.

The principle of our approach is to obtain a mean distance d related to the inter center distances b_{pq}. Let us introduce $\mathbb{L}^1_{\text{eqv}}$ as the matrix of size $M \times M$ defined by

$$\forall p,q = 1,\dots,M, \qquad (\mathbb{L}^1_{\text{eqv}})^{p,q} = \begin{cases} -a\left[\ln\left(\dfrac{ka}{2}\right)+\gamma\right] + i\dfrac{\pi a}{2}, & \text{for } p = q, \\ -a\left[\ln\left(\dfrac{kd}{2}\right)+\gamma\right] + i\dfrac{\pi a}{2}, & \text{for } p \neq q, \end{cases}$$

where $d > 0$ is an "equivalent" distance related to the distances b_{pq} (the coefficients $(\mathbb{L}^1_{\text{eqv}})^{p,q}$ are obtained by replacing b_{pq} by d in (25)). We suppose that d satisfies the inequality

$$d \geq \min_{1 \leq p \neq q \leq M} b_{pq}. \tag{26}$$

Let us remark that the matrix $\mathbb{L}^1_{\text{eqv}}$ is defined through two parameters by

$$\mathbb{L}^1_{\text{eqv}} = \begin{pmatrix} l_0 & l_1 & l_1 & \dots & l_1 \\ l_1 & l_0 & l_1 & \dots & l_1 \\ l_1 & l_1 & l_0 & \dots & l_1 \\ \vdots & \ddots & \ddots & \ddots & \vdots \\ l_1 & \dots & l_1 & l_1 & l_0 \end{pmatrix},$$

with

$$\begin{cases} l_0 = (\mathbb{L}^1_{\text{eqv}})^{0,0} = -a\left[\ln\left(\dfrac{ka}{2}\right)+\gamma\right] + i\dfrac{\pi a}{2}, \\ l_1 = (\mathbb{L}^1_{\text{eqv}})^{1,1} = -a\left[\ln\left(\dfrac{kd}{2}\right)+\gamma\right] + i\dfrac{\pi a}{2}. \end{cases} \tag{27}$$

The main property of this matrix is that we explicitly know its eigenvalues, and most particularly its largest one, accordingly to the next Lemma.

Lemma 4. *The eigenvalues of* $\mathbb{L}^1_{\text{eqv}}$ *are given by*

- $\mu^1_1 = l_0 + (M-1)l_1 = -a\left[\ln\left(\dfrac{ka}{2}\right) + (M-1)\ln\left(\dfrac{kd}{2}\right)\right] - aM\gamma + i\dfrac{M\pi a}{2}$, *with multiplicity* 1,
- $\mu^1_2 = l_0 - l_1 = a\ln\left(\dfrac{d}{a}\right)$, *with multiplicity* $(M-1)$.

Moreover, for $kd < 1$, *we have the following inequality*

$$\left|\mu^1_1\right| \geq \left|\mu^1_2\right|. \tag{28}$$

Proof. The characteristic polynomial of $\mathbb{L}^1_{\rm eqv}$ is given by: $P(X) = det(\mathbb{L}^1_{\rm eqv} - X\mathbb{I})$, where $\mathbb{I}$ is the $M \times M$ identity matrix,

$$\det(\mathbb{L}^1_{\rm eqv} - X\mathbb{I}) = \det \begin{pmatrix} l_0 - X & l_1 & l_1 & \dots & l_1 \\ l_1 & l_0 - X & l_1 & \dots & l_1 \\ l_1 & l_1 & l_0 - X & \dots & l_1 \\ \vdots & \ddots & \ddots & \ddots & \vdots \\ l_1 & \dots & l_1 & l_1 & l_0 - X \end{pmatrix}.$$

By substracting the first row to rows $2, 3, \dots, M$, and next adding to the first column the other $M-1$ columns, we easily obtain the expression

$$\det(\mathbb{L}^1_{\rm eqv} - X\mathbb{I}) = (-1)^M \left[X - (l_0 + (M-1)l_1)\right] \left[X - (l_0 - l_1)\right]^{M-1}.$$

We then deduce the eigenvalues of $\mathbb{L}^1$

$$\mu^1_1 = l_0 + (M-1)l_1 = -a\left[\ln\left(\frac{ka}{2}\right) + (M-1)\ln\left(\frac{kd}{2}\right)\right] - aM\gamma + i\frac{M\pi a}{2},$$

with multiplicity 1, and $\mu^1_2 = l_0 - l_1 = a\ln\left(\frac{d}{a}\right)$, with multiplicity $M-1$.

Let us now state the inequality (28). We first remark that the eigenvalue μ^1_2 is real. From relation (27) and since $d > a$, μ^1_2 is positive. It remains to prove that the real part of μ^1_1 is larger than μ^1_2. Let first remark that $\mu^1_2 = \Re(l_0) - \Re(l_1)$ since μ^1_2 is real. We next compare the real part of μ^1_1 with μ^1_2:

$$\Re(\mu^1_1) - \mu^1_2 = (M-2)\Re(l_1). \tag{29}$$

Since $M - 2 \geq 0$, $\Re(\mu^1_1) - \mu^1_2$ and $\Re(l_1)$ have the same sign. Let us prove that $\Re(l_1)$ is positive. The real part of l_1 is: $\Re(l_1) = -a\left[\ln\left(\frac{kd}{2}\right) - \gamma\right]$. Let us recall that: $-\ln(0.5) \simeq 0.69 > \gamma \simeq 0.58$. We assume that we have $kd < 1$ (since k tends towards 0). Since ln is an increasing function, we get: $-\ln\left(\frac{kd}{2}\right) > \gamma > 0$, that is $\Re(l_1) = a\left[-\ln\left(\frac{kd}{2}\right) - \gamma\right] \geq 0$. By using (29), we have $\Re(\mu^1_1) - \mu^1_2 \geq 0$, and next $\left|\mu^1_1\right| \geq \left|\mu^1_2\right|$. □

This Lemma shows that the eigenvalue $\mu^{1,\rm eqv}_{max}$ of $\mathbb{L}^1_{\rm eqv}$ with largest modulus has a multiplicity equal to 1 and is given by

$$\mu^{1,\rm eqv}_{max} = l_0 + (M-1)l_1 = -a\left[\ln\left(\frac{ka}{2}\right) + (M-1)\ln\left(\frac{kd}{2}\right)\right] - aM\gamma + i\frac{M\pi a}{2}. \tag{30}$$

We now estimate μ_{max} by $\mu^{1,\rm eqv}_{max}$, that is

$$\mu_{max} \simeq -a\left[\ln\left(\frac{ka}{2}\right) + (M-1)\ln\left(\frac{kd}{2}\right)\right] - aM\gamma + i\frac{M\pi a}{2}.$$

We propose to choose d as: $d = \frac{b_{min}+b_{max}}{2}$. The term b_{min}, respectively b_{max}, represents the smallest, respectively largest, possible distance b_{pq} between the centers of two obstacles. When the obstacles are contained in a rectangular box of sides ℓ and L, we fix b_{min} and b_{max} as: $b_{min} = 2a$ and $b_{max} = \sqrt{\ell^2 + L^2} - 2a$. Finally, d is defined as the average of b_{min} and b_{max}

$$d = \frac{b_{min} + b_{max}}{2} = \frac{\sqrt{\ell^2 + L^2}}{2}. \tag{31}$$

Let us remark that d can also be seen as the half diagonal of the box with sidelenghts ℓ and L. Let us come back again to the example presented in Figure 3. The numerical computation of the largest eigenvalue μ_{max} of $\mathbb{L}$ was $\mu_{max} \simeq 5.39 + 4.62i$, with $|\mu_{max}| \simeq 7.1$. By using relation (31) for d, one gets $d = 2\sqrt{2}$. The proposed formula (30) then gives $\mu_{max}^{1,\text{eqv}} \simeq 4.47 + 4.71i$, with $|\mu_{max}^{1,\text{eqv}}| \simeq 6.5$. The relative error when estimating μ_{max} by $\mu_{max}^{1,\text{eqv}}$ is then equal to

$$100 \frac{\left| \mu_{max} - \mu_{max}^{1,\text{eqv}} \right|}{|\mu_{max}|} = 13.04\%, \tag{32}$$

and, in term of the modulus, to

$$100 \frac{\left| |\mu_{max}| - \left| \mu_{max}^{1,\text{eqv}} \right| \right|}{|\mu_{max}|} = 8.4\%, \tag{33}$$

which means that our approach is consistent. Moreover, let us point out that, unlike the dilute medium case [6], we propose here an estimate of the eigenvalue μ_{max} and not only of its modulus. We launched 100 tests respecting the same parameters set ($k = 0.1$, $N = 5$, 30 randomly distributed disks of radius 0.1 in $[0, 4]^2$ with $b_{pq} \geq 0.1$). We observe on Figures 4(a) and 4(b) that the error essentially affects the real part of μ_{max} while the estimate of the imaginary part is acceptable. The average relative error on the modulus of μ_{max} for these 100 realizations is about 15.6%.

3.4 Condition number estimate

Like in the dilute medium case [6], the condition number $\text{cond}_2(\mathbb{L})$ of the matrix $\mathbb{L}$ is estimated by the quantity

$$\left| \frac{\mu_{max}}{\mu_{min}} \right|. \tag{34}$$

Thus, an approximate condition number $\text{cond}_{app}(\mathbb{L})$ is obtained by replacing μ_{min} and μ_{max} by their respective estimates (24) and (30) in Equation (34)

$$\text{cond}_2(\mathbb{L}) \simeq \text{cond}_{app}(\mathbb{L}) = 2N \left| - \left[\ln\left(\frac{ka}{2}\right) + \ln\left(\frac{kd}{2}\right) \right] - M\gamma + i\frac{M\pi}{2} \right|. \tag{35}$$

Let us consider again the example of Figure 3. Then, the numerical condition number of $\mathbb{L}$ is: $\text{cond}_2(\mathbb{L}) \simeq 713$ while the estimate (35) yields $\text{cond}_{app}(\mathbb{L}) \simeq 650$, leading to a relative error

$$100 \frac{|\text{cond}_2(\mathbb{L}) - \text{cond}_{app}(\mathbb{L})|}{|\text{cond}_2(\mathbb{L})|} \simeq 9\%. \tag{36}$$

Essentially, this error is related to the estimate of the largest eigenvalue. We report on Figure 5 the results for 100 launches. This gives a mean relative error equal to 11%, which is satisfactory.

4 Connections with the boundary element approximation and extension to other geometries

We approximate the single-layer potential by a linear boundary element method. For more details we refer to [6] where a similar approach is developed for distant obstacles. The boundary Γ (which is

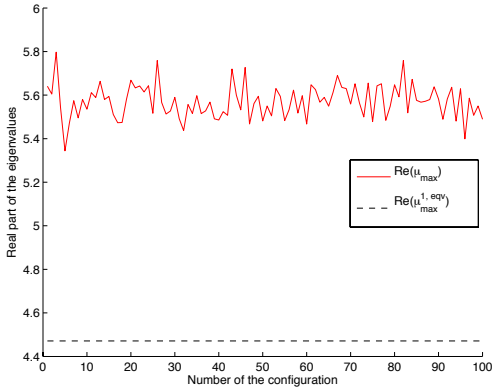

(a) Real parts of μ_{max} and $\mu_{max}^{1,\mathrm{eqv}}$

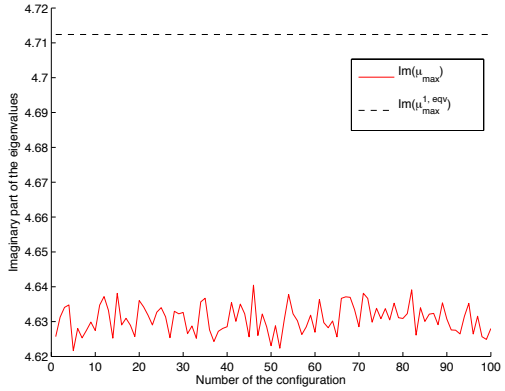

(b) Imaginary parts of μ_{max} and $\mu_{max}^{1,\mathrm{eqv}}$

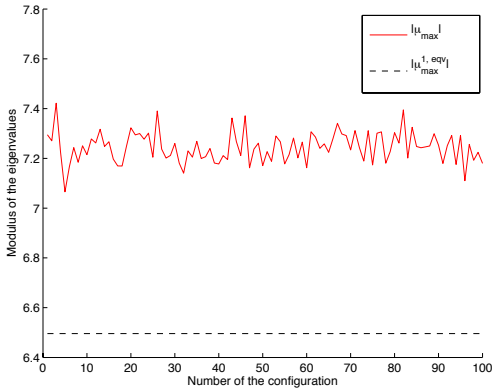

(c) Modulii of μ_{max} and $\mu_{max}^{1,\mathrm{eqv}}$

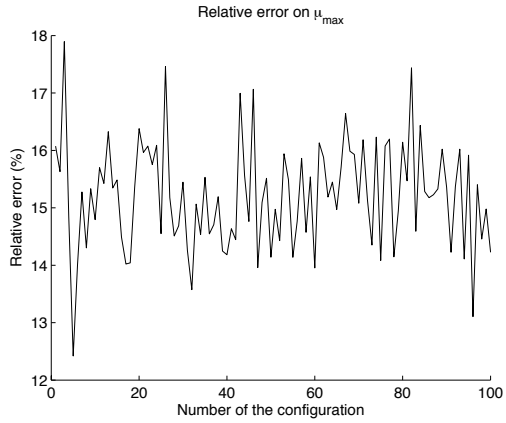

(d) Relative error (%) given by relation (32) on μ_{max}

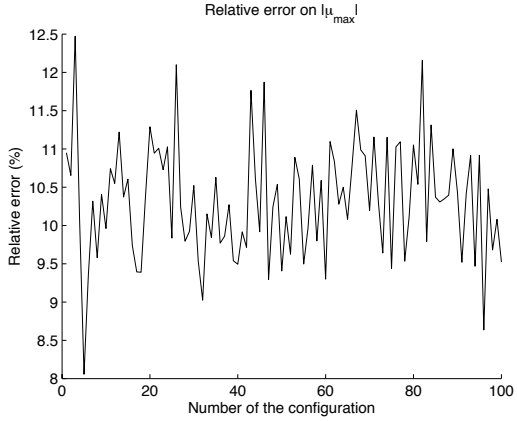

(e) Relative error (%) given by relation (33) on the modulus of μ_{max}

Figure 4: Comparisons between μ_{max} and its estimate $\mu_{max}^{1,\mathrm{eqv}}$ for 100 configurations of $M = 30$ obstacles with radius $a = 0.1$ randomly placed in $[0, 4]^2$, with $k = 0.1$, $N = 5$ and $b \geq 0.3 (= 3a)$.

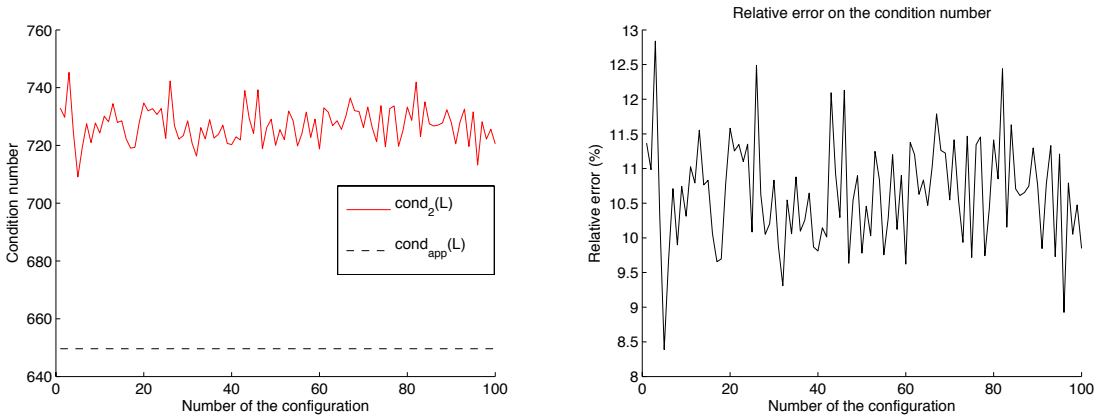

(a) Comparison between the exact and approximate condition numbers

(b) Relative error on the condition number (%) (see relation (36))

Figure 5: Comparison between the exact and approximate condition numbers of $\mathbb{L}$, for 100 configurations of $M = 30$ disks with radius $a = 0.1$ randomly distributed in $[0, 4]^2$ ($k = 0.1$, $N = 5$, $b \geq 0.3(= 3a)$).

the union of the M boundaries Γ_p) is approximated by polygonal curves Γ_h, where h designates the smallest element size of the $N_{tot,h}$ segments composing Γ_h. The boundary element space V_h is the space of piecewise linear elements on each segment of Γ_h. Let us introduce $[L_h] \in \mathcal{M}_{N_{tot,h},N_{tot,h}}(\mathbb{C})$ as the single-layer matrix and $[M_h] \in \mathcal{M}_{N_{tot,h},N_{tot,h}}(\mathbb{C})$. as the global mass matrix for linear finite element. Finally, we denote by μ^h_{min}, respectively μ^h_{max}, the eigenvalue of $[M_h]^{-1}[L_h]$ with the smallest, respectively largest, modulus.

4.1 The circular cylinder case

As in [6], we begin by considering the case of circular cylinders and then formally extend the results to rectangular and elliptical shaped objects. We consider M disks Ω_p with the same radius a and we uniformly mesh each circle Γ_p by fixing the meshsize to h. Following [6], we formally substitute N by $\pi a h^{-1} - 1/2$ in the estimate (24), respectively (30), of μ_{min}, respectively μ_{max}. When k tends towards 0, we therefore obtain $\mu_{min} \simeq \mu^{app}_{min}(a, h)$ and $\mu_{max} \simeq \mu^{app}_{max}(a, k)$, with

$$\begin{cases} \mu^{app}_{min}(a,h) = \dfrac{a}{2\pi a h^{-1} - 1}, \\ \\ \mu^{app}_{max}(a,k) = -a\left[\ln\left(\dfrac{ka}{2}\right) + (M-1)\ln\left(\dfrac{kd}{2}\right)\right] - aM\gamma + i\dfrac{M\pi a}{2}, \end{cases} \tag{37}$$

where d represents a mean distance between obstacles. When the obstacles are contained in the rectangular box $[0, \ell] \times [0, L]$, we use the previous expression (31): $d = \frac{\sqrt{\ell^2+L^2}}{2}$. In addition, when k tends towards zero, the condition number of the matrix $[M_h]^{-1}[L_h]$ is approximated by

$$\mathrm{cond}(k, a, \Gamma_h) := \mathrm{cond}_2([M_h]^{-1}[L_h]) \simeq \mathrm{cond}_{app}(k, a, h),$$

with

$$\mathrm{cond}_{app}(k, a, h) = a(2\pi a h^{-1} - 1)\left|-\ln\left(\frac{ka}{2}\right) - (M-1)\ln\left(\frac{kd}{2}\right) - M\gamma + i\frac{M\pi}{2}\right|. \tag{38}$$

We propose to numerically validate the above approximations for the preceeding example: $M = 30$ small disks of radius $a = 0.1$ are placed inside the box $[0, 4]^2$. The smallest inter centers distance b is equal to $0.3(= 3a)$ and $k = 0.1$. Moreover, each obstacle is meshed with $N_h = 50$ elements. We numerically compute the eigenvalues and the condition number of $[M_h]^{-1}[L_h]$ for 100 configurations as well as their corresponding estimates. Let us begin by comparing the numerical (μ^h_{min} and μ^h_{max}) and estimated eigenvalues on Figures 6 and 7. According to Figure 6, the relative error on the smallest eigenvalue μ^h_{min} is about 2.4%, which is very satisfactory and similar to the distant obstacles case [6]. Concerning the largest eigenvalue, on Figure 7, the relative error is about 15%, the main deterioration being on the real part of μ^h_{max}. Moreover, the mean relative error on the modulus of μ^h_{max} is about 10%. By comparison, we get similar errors with the spectral method. We compare now on Figure 8 the variations of the condition number of $[M_h]^{-1}[L_h]$ with its estimate (38). We obtain a mean relative error of 13% which is about the same as for the spectral method (11%).

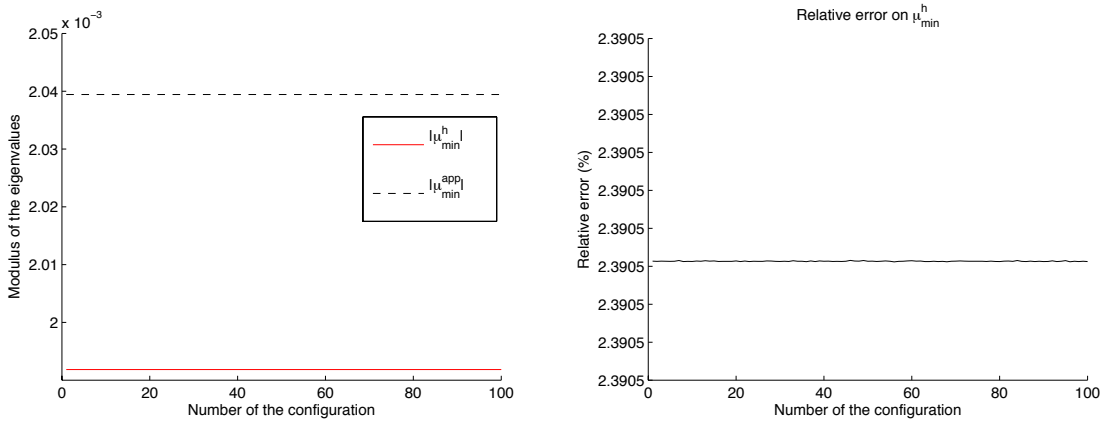

(a) Comparison between the moduli of the smallest eigenvalue and its estimate (37)

(b) Relative error on the modulus of μ_{min}

Figure 6: Comparison of the smallest eigenvalue μ^h_{min} of the matrix $[M_h]^{-1}[L_h]$ and its estimate (37). The obstacles are small disks of radius $a = 0.1$ discretized by using $N_h = 50$ segments. For each of the 100 configurations, we randomly place $M = 30$ disks in $[0, 4]^2$, with $k = 0.1$ and $b \geq 0.3(= 3a)$.

4.2 Extension to other geometries

We now formally adapt the estimates (37) first to elliptical and then to rectangular cylinders. We proceed as [6]: we formally replace the radius a and the meshsize h in the estimates (37) by respectively an equivalent radius a_{eqv} and an equivalent step h_{eqv}. For an ellipse with semi-axis a_{x_1} along the direction x_1 and a_{x_2} along x_2, we proposed to choose an equivalent mesh parameter h_{eqv} equal to the smallest discretization meshsize. Moreover the three equivalent radii were considered

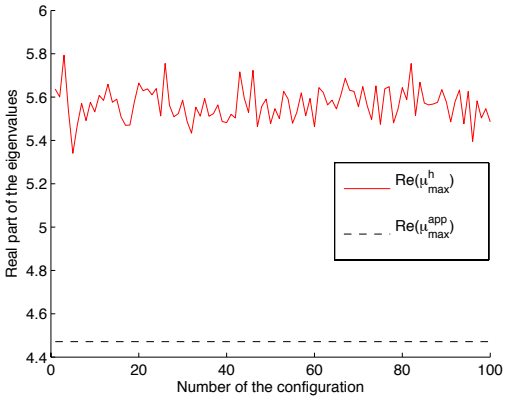

(a) Comparison between the real part of the largest eigenvalue and its estimate (37)

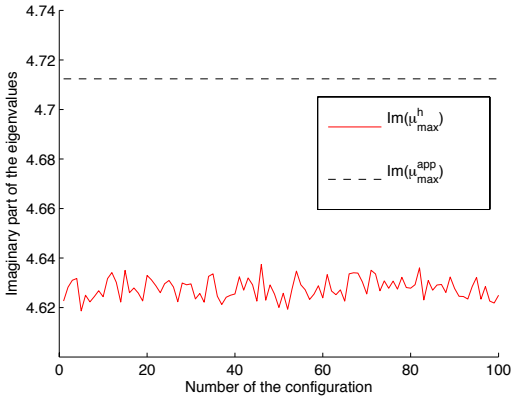

(b) Comparison between the imaginary part of the largest eigenvalue and its estimate (37)

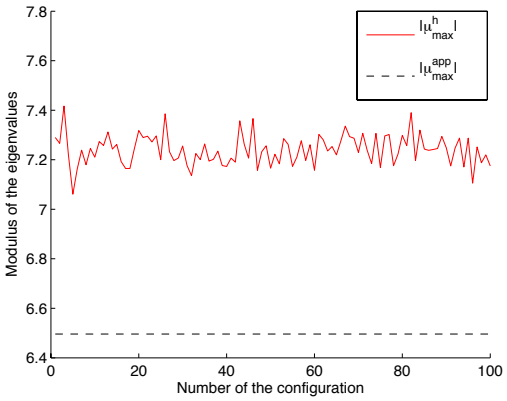

(c) Comparison between the moduli of the largest eigenvalue and its estimate (37)

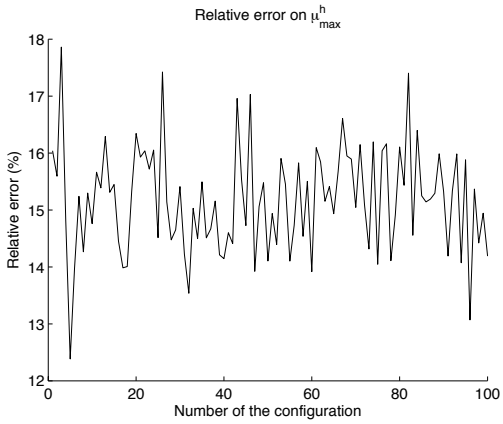

(d) Relative error on μ_{max}

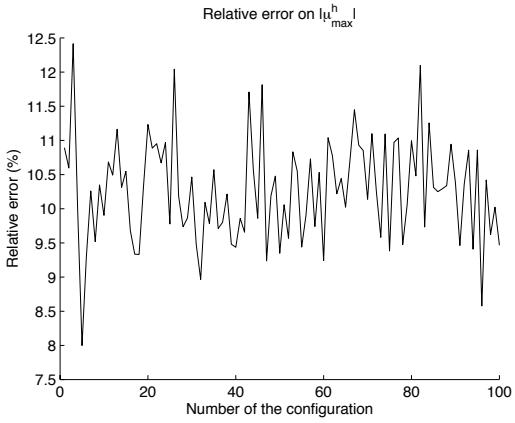

(e) Relative error on the modulus of μ_{max}

Figure 7: Largest eigenvalue μ^h_{max} of the matrix $[M_h]^{-1}[L_h]$ and its estimate (37). The obstacles are small disks of radius $a = 0.1$ discretized by using $N_h = 50$ segments. For each of the 100 configurations, we randomly place $M = 30$ disks in $[0, 4]^2$, with $k = 0.1$ and $b \geq 0.3(= 3a)$.

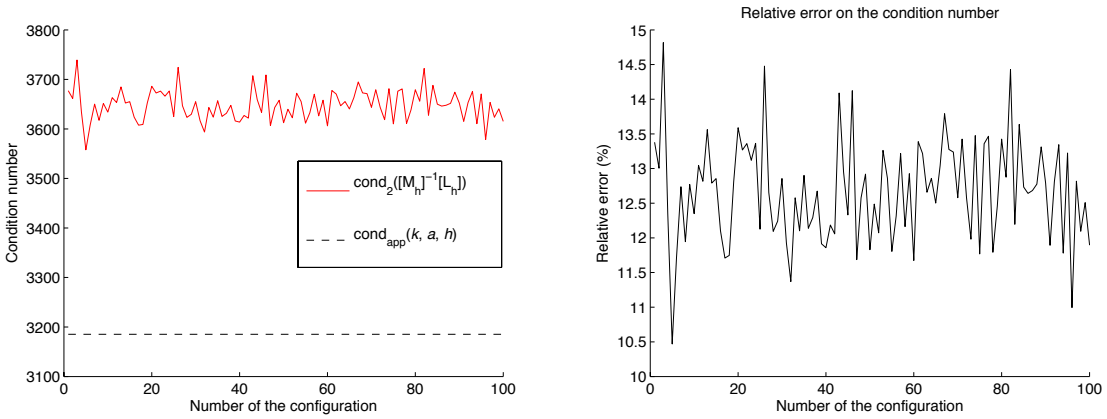

(a) Comparison between the exact and approximate condition numbers

(b) Relative error on the conditioning

Figure 8: Comparison between the condition number of the matrix $[M_h]^{-1}[L_h]$ and its estimate (38). The obstacles are small disks of radius $a = 0.1$ discretized by using $N_h = 50$ segments. For each of the 100 configurations, $M = 30$ disks are randomly placed in $[0, 4]^2$, with $k = 0.1$ and $b \geq 0.3 (= 3a)$.

[6]

$$a^1_{\text{eqv}} = \frac{a_{x_1} + a_{x_2}}{2}, \qquad a^2_{\text{eqv}} = \frac{2a_{x_1}a_{x_2}}{a_{x_1} + a_{x_2}} \qquad \text{et} \qquad a^3_{\text{eqv}} = \frac{\sqrt{a^2_{x_1} + a^2_{x_2}}}{\sqrt{2}}.$$

We propose to validate these approximations for small ellipses with semi-axes $a_{x_1} = 0.1$ and $a_{x_2} = 0.025$. We keep the same parameters as before (30 obstacles randomly placed in $[0, 4]^2$, with $k = 0.1$ and $b \geq 0.3 (= 3a_{x_1})$, where b is the smallest distance between the centers of two ellipses). We numerically compute the smallest and largest eigenvalues of $[M_h]^{-1}[L_h]$ as well as its condition number for 100 configurations. Figures 9 and 10 compare the eigenvalues μ^h_{min} and μ^h_{max} with their estimates while Figure 11 reports the condition number and its estimate. Let us remark that the numerical simulations show that choosing a^2_{eqv} leads to an inaccurate approximation of the eigenvalues. For the sake of clarity, we only present the results obtained for the two other equivalent radii a^1_{eqv} and a^3_{eqv}. We begin by comparing the estimates of μ^h_{min} and μ^h_{max} on Figures 9 and 10. Like for the single scattering situation [6], choosing an equivalent radius has almost no effect on the estimate of μ^h_{min}. Furthermore, the relative error on μ^h_{min} is of the order of 18%, for each radius (see Figure 9(b)). This important error can be explained by the fact that μ^h_{min} is strongly mesh dependent, and most particularly relatively to the smallest mesh size (strong curvature effects). Hence, the estimate of the smallest eigenvalue can clearly degenerate. Concerning the eigenvalue with largest modulus μ^h_{max}, it is directly impacted by the choice of the equivalent radius. Indeed, Figure 7 shows that a^3_{eqv} leads to a better approximation of μ_{max} than a^1_{eqv}. More precisely, the mean relative error on μ^h_{max} is about 14% for a^3_{eqv} compared with 22% for a^1_{eqv}. On the other hand, the estimates of the modulus of μ^h_{max} are more precise with a mean relative error of about 5.4% for a^3_{eqv} compared with 19% for a^1_{eqv}. When the obstacles are distant, we observed the opposite behavior [6]. Finally, we compare on Figure 11 the condition number of the matrix $[M_h]^{-1}[L_h]$ with its estimate. We have only reported the results related to a^3_{eqv} since it leads to the best

approximation of μ^h_{max}. The relative error on the condition number is about 9% which is very satisfactory.

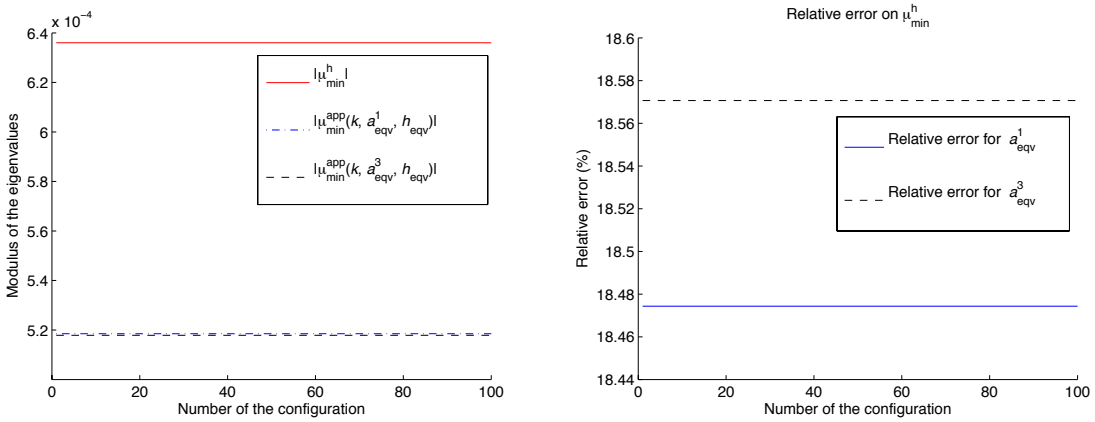

(a) Comparison between the moduli of the smallest eigenvalue and its estimates

(b) Relative error on the modulus of μ_{min}

Figure 9: Comparison of the estimates (37) of the smallest eigenvalues μ^h_{min} of $[M_h]^{-1}[L_h]$. The obstacles are small ellipses with semi axis $a_{x_1} = 0.1$ and $a_{x_2} = 0.025$, obtained for a discretization with $N_h = 50$ segments. For each of the 100 configurations, $M = 30$ ellipses are randomly distributed in $[0,4]^2$, setting $k = 0.1$ and $b \geq 0.3 (= 3a_{x_1})$.

We end this numerical study by considering rectangular obstacles with half side lengths a_{x_1} and a_{x_2}. We take the equivalent radius a^4_{eqv} given by [6]: $a^4_{\text{eqv}} = \frac{(1+\sqrt{2})}{2}\frac{\sqrt{a^2_{x_1}+a^2_{x_2}}}{\sqrt{2}}$. Moreover, the equivalent step h_{eqv} is always chosen equal to the smallest discretization meshsize $h_{\text{eqv}} = \min_{1\leq p\leq M}\min_{1\leq j\leq N_{h,p}} h_{p,j}$. We provide a numerical example considering the previous parameters: $M = 30$ randomly placed rectangular cylinders with half side lengths $a_{x_1} = 0.1$ and $a_{x_2} = 0.025$ in $[0,4]^2$. Moreover, we set $k = 0.1$ and $b \geq 0.3 (= 3a_{x_1})$. Numerically, we compute the eigenvalues of the matrix $[M_h]^{-1}[L_h]$, its condition number as well as their respective estimates for 100 configurations. We begin by comparing on Figure 12, respectively Figure 13, the estimates of the eigenvalues with smallest, respectively largest, modulus μ^h_{min}, respectively μ^h_{max}. The average relative error on μ^h_{min} is 2%, compared with 18% in the elliptical case. This can be explained by the property that, in the rectangular case, the mesh is non uniform but the mesh size is constant on each of the four rectangle sides (unlike the ellipse). Concerning the eigenvalue with largest modulus μ^h_{max}, the relative error is about 13%, which is of the same order as for disks and ellipses, and about 2.4% on its modulus, which is very precise. Finally, the condition number estimate is satisfactory since, from Figure 14, the average relative error is about 14% like for disks.

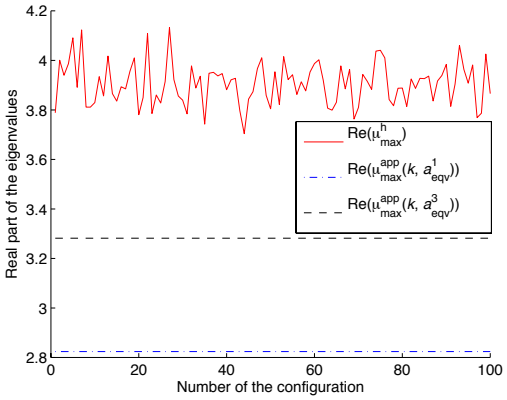

(a) Comparison between the real part of the largest eigenvalue and its estimates (37)

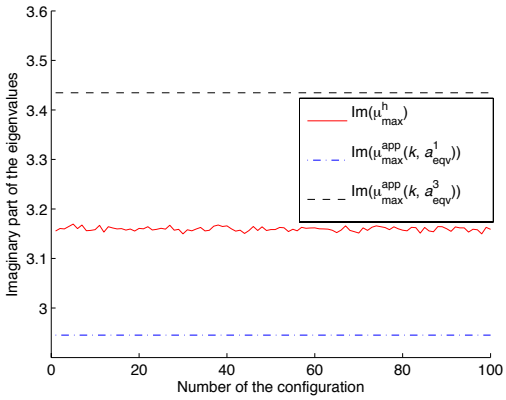

(b) Comparison between the imaginary part of the largest eigenvalue and its estimates (37)

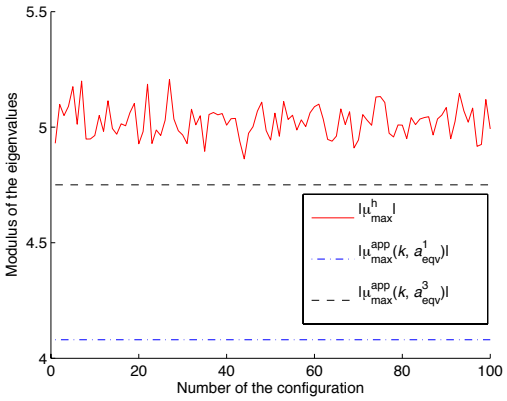

(c) Comparison between the moduli of the largest eigenvalue and its estimates (37)

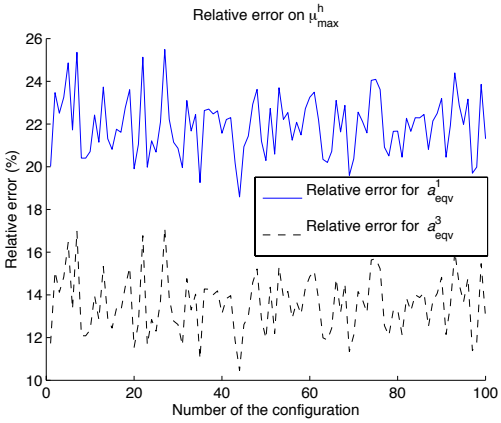

(d) Relative error on the modulus of μ_{max}

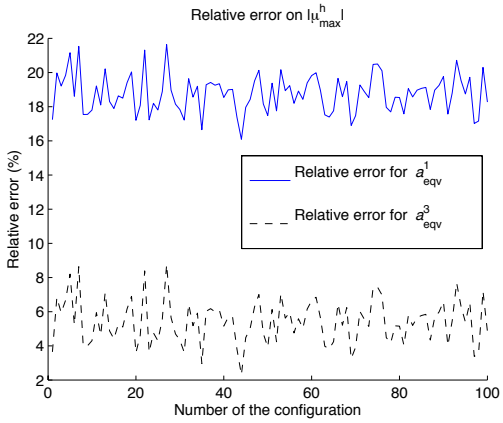

(e) Relative error on the modulus of μ_{max}

Figure 10: Comparison of the estimates (37) of the largest eigenvalues μ^h_{max} of $[M_h]^{-1}[L_h]$. The obstacles are small ellipses with semi axis $a_{x_1} = 0.1$ and $a_{x_2} = 0.025$, obtained for a discretization with $N_h = 50$ segments. For each of the 100 configurations, $M = 30$ ellipses are randomly distributed in $[0, 4]^2$, setting $k = 0.1$ and $b \geq 0.3 (= 3a_{x_1})$.

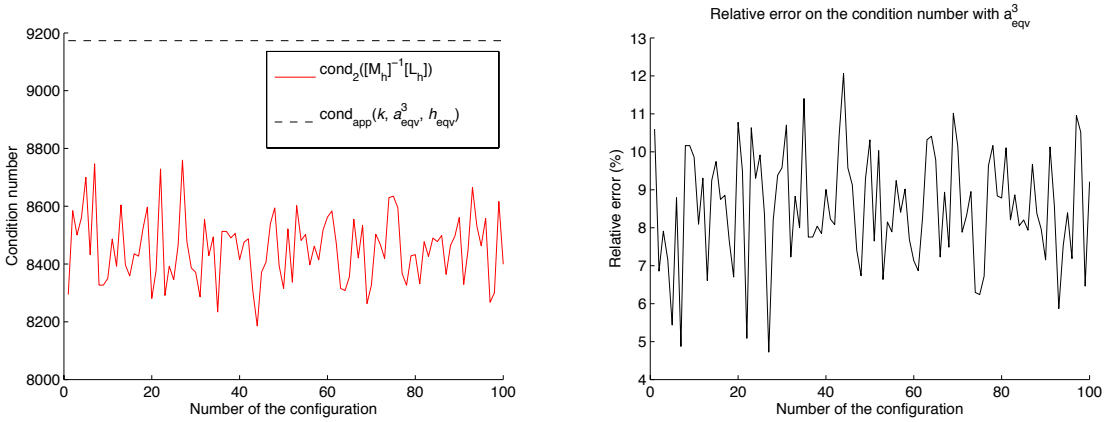

(a) Comparison between the exact and approximate condition numbers

(b) Relative error on the condition number

Figure 11: Comparison between the condition number of the matrix $[M_h]^{-1}[L_h]$ and its estimate. The obstacles are ellipses with semi-axis $a_{x_1} = 0.1$ and $a_{x_2} = 0.025$, discretized with $N_h = 50$ segments. For each of the 100 configurations, $M = 30$ ellipses are randomly distributed in $[0, 4]^2$, with $k = 0.1$ and $b \geq 0.3 (= 3a_{x_1})$.

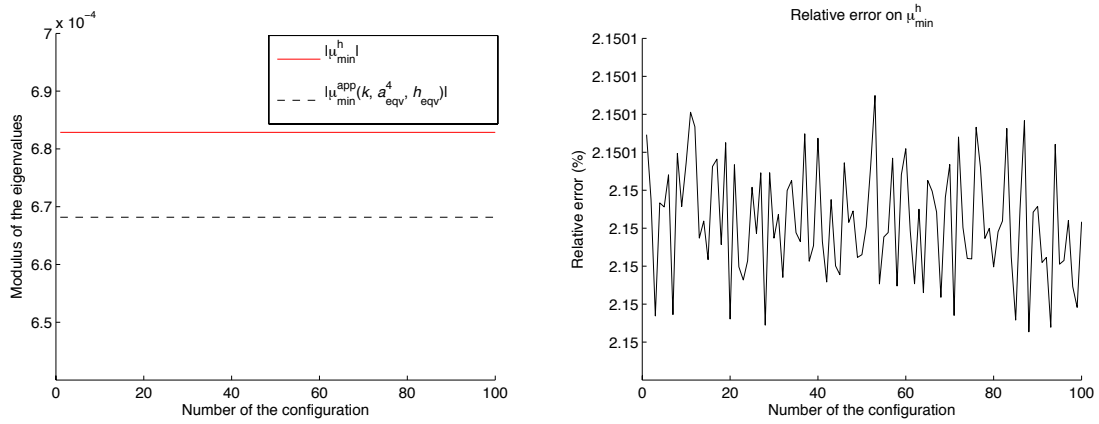

(a) Comparison between the moduli of the smallest eigenvalue and its estimate

(b) Relative error on the modulus of μ_{min}

Figure 12: Smallest eigenvalue μ^h_{min} of the matrix $[M_h]^{-1}[L_h]$ and its estimate (37) for rectangular cylinders with half side lengths $a_{x_1} = 0.1$ and $a_{x_2} = 0.025$. Each rectangle is discretized with $N_h = 48$ segments (12 by edge). For each of the 100 configurations, $M = 30$ rectangular cylinders are randomly placed in $[0, 4]^2$, with $k = 0.1$ and $b \geq 0.3 (= 3a_{x_1})$.

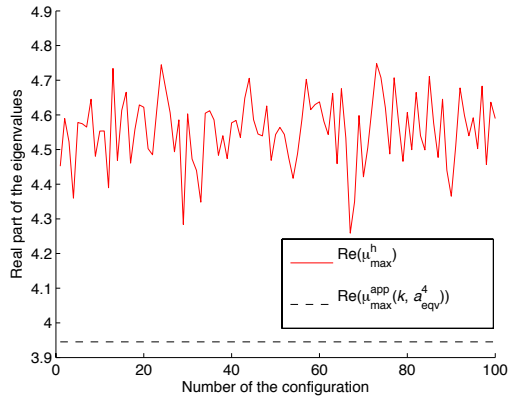

(a) Comparison between the real part of the largest eigenvalue and its estimate

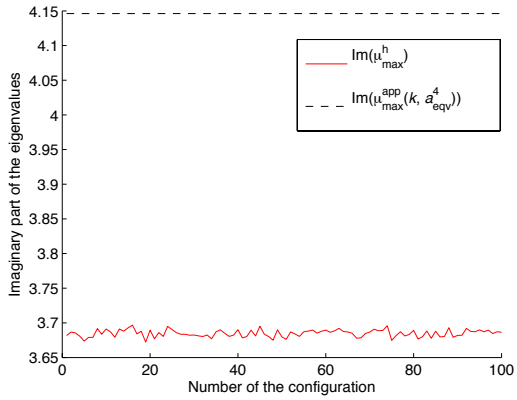

(b) Comparison between the imaginary part of the largest eigenvalue and its estimate

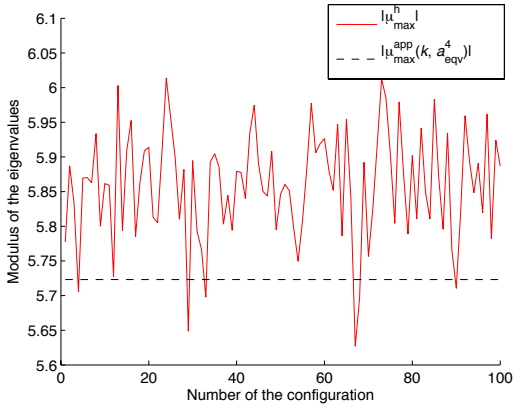

(c) Comparison between the moduli of the largest eigenvalue and its estimate

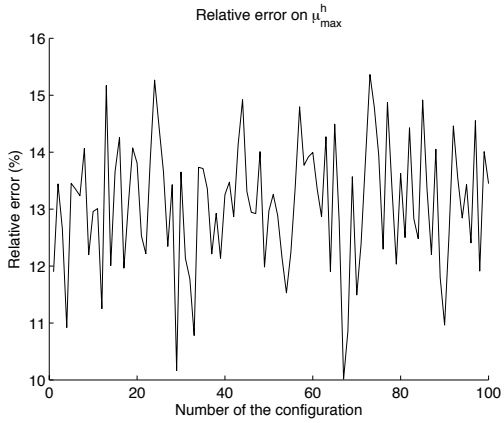

(d) Relative error on μ_{max}

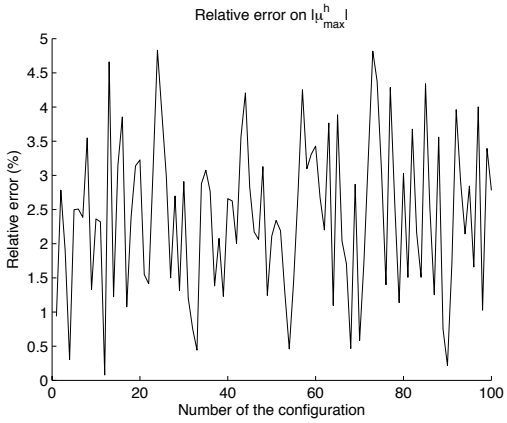

(e) Relative error on the modulus of μ_{max}

Figure 13: Comparison between the largest eigenvalue μ^h_{max} of the matrix $[M_h]^{-1}[L_h]$ and its estimate (37) for rectangular cylinders with half side lengths $a_{x_1} = 0.1$ and $a_{x_2} = 0.025$. Each rectangle is discretized with $N_h = 48$ segments (12 by edge). For each of the 100 configurations, $M = 30$ rectangular cylinders are randomly placed in $[0, 4]^2$, with $k = 0.1$ and $b \geq 0.3(= 3a_{x_1})$.

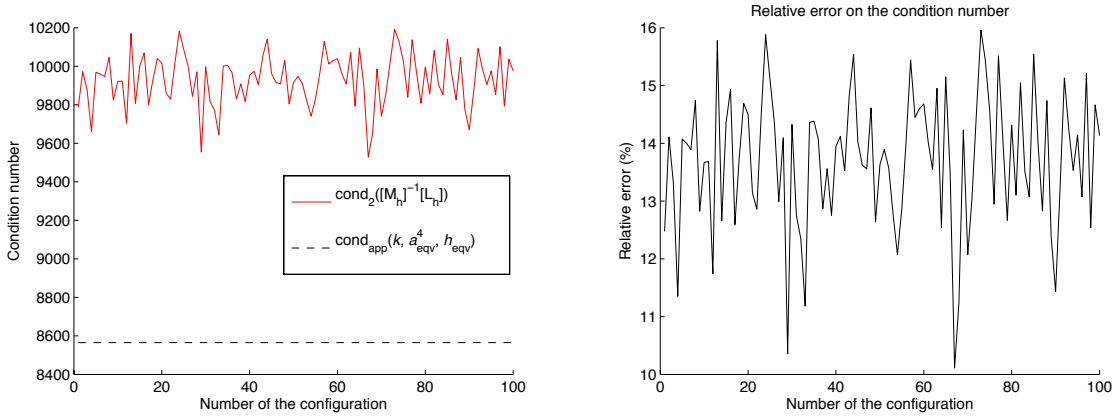

(a) Comparison between the exact and approximate condition numbers

(b) Relative error on the condition number

Figure 14: Comparison between the condition number of the matrix $[M_h]^{-1}[L_h]$ and its estimate. The obstacles are rectangles with half side lengths $a_{x_1} = 0.1$ and $a_{x_2} = 0.025$, each being discretized with $N_h = 48$ elements (12 by edge). For each of the 100 configurations, $M = 30$ rectangles are randomly distributed in $[0, 4]^2$, setting $k = 0.1$ and $b \geq 0.3 (= 3a_{x_1})$.

5 Conclusion

In this second and last part, we developed and validated low-frequency spectral and condition number estimates of the single-layer integral operator for dense multiple scattering media. They have been formally extended to circular, elliptical and rectangular shaped obstacles when a linear boundary element is considered. These estimates provide explicit dependence of the eigenvalues with respect to the different problem parameters.

These studies open different directions which should complete this work. First, spectral estimates related to the Brakhage-Werner integral equation [4, 5, 9] and Combined Field Integral Equation [4, 5, 19] can be expected in similar situations since they involve the four basic integral operators: the single- and double-layer potentials as well as their normal derivatives. A difficult situation that is not studied here is the case where the distance between the obstacles is of the order of the characteristic size of the scatterers. We did not succeed yet in deriving similar estimates. One of the main difficulties is that an asymptotic regime is not available. Finally, considering the medium/high frequency as well as three-dimensional case are of interest but require further studies.

References

[1] M. Abramowitz and I.A. Stegun. *Handbook of Mathematical Functions with Formulas, Graphs, and Mathematical Tables*. New York: Dover Publications, Ninth Printing (1972).

[2] X. Antoine, A. Bendali, and M. Darbas. Analytic preconditioners for the electric field integral equation. *Internat. J. Numer. Methods Engrg.*, (61):1310–1331, 2004.

[3] X. Antoine, A. Bendali, and M. Darbas. Analytic preconditioners for the boundary integral solution of the scattering of acoustic waves by open surfaces. *J. Comput. Acoust.*, 3(13):477–498, 2005.

[4] X. Antoine and M. Darbas. Alternative integral equations for the iterative solution of acoustic scattering problems. *Quaterly J. Mech. Appl. Math.*, 1(58):107–128, 2005.

[5] X. Antoine and M. Darbas. Generalized Combined Field Integral Equations for the iterative solution of the three-dimensional Helmholtz equation. *M2AN Math. Model. Numer. Anal.*, 1(41):147–167, 2007.

[6] X. Antoine and B. Thierry. Spectral and condition number estimates of the acoustic single-layer operator for low frequency multiple scattering in dilute media. *submitted*, 2011.

[7] T. Betcke, S.N. Chandler-Wilde, I.G. Graham, S. Langdon, and M. Lindner. Condition number estimates for combined potential operators in acoustics and their boundary element discretisation. *Numer. Methods Partial Differential Eq.*, to appear, 2011.

[8] S. Bidault, F.J.G. de Abajo, and A. Polman. Plasmon-based nanolenses assembled on a well-defined DNA template. *Journal of the American Chemical Society*, 130(9):2750+, 2008.

[9] H. Brakhage and P. Werner. Über das Dirichletsche Aussenraumproblem für die Helmholtzsche Schwingungsgleichung. *Arch. Math.*, 16:325–329, 1965.

[10] S.N. Chandler-Wilde, I.G. Graham, S. Langdon, and M. Lindner. Condition number estimates for combined potential boundary integral operators in acoustic scattering. *J. Integral Equations Appl.*, (21):229–279, 2009.

[11] W.C. Chew and K.F. Warnick. On the spectrum of the electric field integral equation and the convergence of the moment method. *Internat. J. Numer. Methods Engrg.*, (51):475–489, 2001.

[12] D. L. Colton and R. Kress. *Integral Equation Methods in Scattering Theory*. Pure and Applied Mathematics (New York). John Wiley & Sons Inc., New York, 1983. A Wiley-Interscience Publication.

[13] E Darve. The fast multipole method: Numerical implementation. *Journal of Computational Physics*, 160(1):195–240, 2000.

[14] A. Devilez, N. Bonod, J. Wenger, D. Gerard, B. Stout, H. Rigneault, and E. Popov. Three-dimensional subwavelength confinement of light with dielectric microspheres. *Optics Express*, 17(4):2089–2094, 2009.

[15] A. Devilez, B. Stout, N. Bonod, and E. Popov. Spectral analysis of three-dimensional photonic jets. *Optics Express*, 16(18):14200–14212, 2008.

[16] T.E. Doyle, A.T. Tew, K.H. Warnick, and B.L. Carruth. Simulation of elastic wave scattering in cells and tissues at the microscopic level. *Journal of the Acoustical Society of America*, 125(3):1751–1767, 2009.

[17] P. Ferrand, J. Wenger, A. Devilez, M. Pianta, B. Stout, N. Bonod, E. Popov, and H. Rigneault. Direct imaging of photonic nanojets. *Optics Express*, 16(10):6930–6940, 2008.

[18] L Greengard and V Rokhlin. A Fast Algorithm for Particle Simulation. *Journal of Computational Physics*, 73(2):325–348, 1987.

[19] R.F. Harrington and J.R. Mautz. H-field, E-field and combined field solution for conducting bodies of revolution. *Archiv Elektronik und Uebertragungstechnik*, 4(32):157–164, 1978.

[20] P. Hewageegana and V. Apalkov. Second harmonic generation in disordered media: Random resonators. *Physical Review B*, 77(7), 2008.

[21] R.D. Meade J.D. Joannopoulos and Joshua N. Winn. *Photonic Crystals: Molding the Flow of Light*. 1995.

[22] R. Kress. Minimizing the condition number of boundary integral operators in acoustic and electromagnetic scattering. *Quart. J. Mech. Appl. Math.*, 38(2):323–341, 1985.

[23] R. Kress and W. T. Spassov. On the condition number of boundary integral operators for the exterior Dirichlet problem for the Helmholtz equation. *Numer. Math.*, 42(1):77–95, 1983.

[24] K.H. Ding L. Tsang, J.A. Kong and C.O. Ao. *Scattering of Electromagnetic Waves, Numerical Simulation*. Wiley Series in Remote Sensing. J.A. Kong, Series Editor, 2001.

[25] P. A. Martin. *Multiple Scattering. Interaction of Time-Harmonic Waves with N Obstacles*, volume 107 of *Encyclopedia of Mathematics and its Applications*. Cambridge University Press, Cambridge, 2006.

[26] H. Mertens, A. F. Koenderink, and A. Polman. Plasmon-enhanced luminescence near noble-metal nanospheres: Comparison of exact theory and an improved Gersten and Nitzan model. *Physical Review B*, 76(11), 2007.

[27] J.-C. Nédélec. *Acoustic and Electromagnetic Equations. Integral Representations for Harmonic Problems*, volume 144 of *Applied Mathematical Sciences*. Springer-Verlag, New York, 2001.

[28] K. Niino and N. Nishimura. Preconditioning based on Calderon's formulae for periodic fast multipole methods for Helmholtz' equation. *J. Comp. Phys.*, to appear 2011.

[29] Y. Saad and M. Schultz. GMRES: a generalized minimal residual algorithm for solving non-symmetric linear systems. *SIAM J. Sci. Statist. Comput.*, 7(3):856–869, 1986.

[30] B. Thierry. *Analyse et Simulations Numériques du Retournement Temporel et de la Diffraction Multiple*. PhD thesis, 2011.